April 1985 LRP 240/85

THE TCV TOKAMAK

Project Report 1985

F. Hofmann, F.B. Marcus, S.C. Jardin+
G.A. Collins, R. Gruber, A. Heym, Ch. Hollenstein,
B. Joye, R. Keller, J.B. Lister, Ph. Marmillod,
A. Pochelon, F. Troyon, A.D. Turnbull

+Permanent address : PPL Princeton (USA)

TCV PROPOSAL - CRPP - EPFL

(Tokamak à Configuration Variable)

CONTENTS

EXECUTIVE SUMMARY - TCV PROPOSAL

1. MOTIVATION

The INTOR study has contributed to a better appreciation of the problems which still have to be solved before a realistic assessment of the tokamak as a fusion reactor can be made. Among the problems identified is the existence or not of a limit on toroidal β and, if there is one, where is it located and how it manifests itself. In 1983 a simple scaling law which expressed the β limit in terms of only three parameters was proposed, based on a synthesis of many numerical studies of ideal MHD instabilities [1,2]. It reads

$$\beta < C \frac{I(MA)}{B(T)a(m)} \qquad (1)$$

where I is the current, a the plasma half-width in the equatorial plane and B the toroidal field. The constant C was found to lie between 2.5 and 3.15% when stability to all modes is considered with no provision for an eventual wall stabilization contribution, and around 4.5% when only ballooning modes are considered. The experimental status can be summarized in the following way :

- An operational limit which manifests itself as a limit on β is observed in all tokamaks which have sufficient heating.
- This limit can be disruptive or soft (degradation of confinement) for the same set of external parameters, depending on the mode of operation.
- The maximum values obey the same scaling law (1) with a C never exceeding 3.5% when the beam contribution is included and substantially lower when calculated for the bulk plasma only.
- There is no evidence of any wall stabilization effect on the β limit.

The full implication of this scaling law can only be appreciated when the additional constraint of the current limitation due to disruption is introduced. For a circular plasma cross-section this limit is $q_a \approx 2$, which translates into

$$\beta_{max} \approx 0.8\ C \left(\frac{\pi}{A}\right),$$

where A is the aspect ratio. A ≈ 4-5 is usually quoted as a reasonable value for a reactor, which corresponds to a maximum β of less than 2%.

There are two ways to increase β : find a way to break into some new high β operating range or increase the maximum current.

The many circular cross-section tokamaks in operation or in construction, which have at their disposal a large amount of auxiliary heating, are in a good position to follow the first road. Plasma shaping, another scheme proposed to break the β limit, is part of the future programs of COMPASS and SPICA and the Princeton Bean Experiment PBX. Pushing the current through the q=2 limit by some active control is part of the program of COMPASS. Elongation of the plasma, with or without some shaping, has been proposed for some time as a means to increase the maximum current, based on simple MHD considerations. Very high current densities have been obtained in belt pinches at very high elongations (8/1), but the configuration decayed rapidly and there was no active control of the position and shape. These devices were operated as pinches designed to have good shock heating. TOSCA, ISX-B, D-III and JET have created elongated plasmas in the tokamak mode of operation, demonstrating that such plasmas can be created and held for times much longer than characteristic MHD times. In D-III a current has been maintained in an elongated plasma which had twice the maximum current allowed in a circular plasma of the same width and this led to the record β value of 4.6% of 1982. Another benefit accruing from the increase in current is a parallel increase of the density well documented on D-III and also seen in ISX-B.

We propose to attempt to extend the range of plasma elongation substantially beyond the maximum values of 1.8-2.0 already obtained in tokamaks, to study:

- scenarios for the creation of elongated plasmas
- the possibility of maintaining positional stability and optimize the control system
- the dependence of the maximum current on elongation

- the scaling laws for the confinement time and the density limit at high elongation
- the regime in which the plasma eventually settles in a steady state (monotonic or non-monotonic q profile, minimum internal q, island structure)
- the dependence of the β limit on current.

The first 5 points must be first studied in the ohmic phase. The last point is an essential element but it should be remembered that an estimate of the power needed to test this limit requires the knowledge of the current, in order to know where the limit is expected, and of the confinement time. We make provision for the introduction of RF antennae for some auxiliary heating but we do not propose any specific solution now. A little-known consequence of the scaling law for the density limit and the β limit is that, in low field devices, the β at the density limit in the purely ohmic regime is already a sizeable fraction of the β limit. For example in TCA (B_T = 1.5 T, R = 61 cm, a = 18 cm, $n_{max} \approx 3 \times 10^{14}/q$) the β limit corresponds to an average temperature of only 400 eV when the density is at the limit! If the parallelism in the density and β limits dependence on current remains correct at high elongation, very high β should already be obtainable in the purely ohmic regime, although at relatively low temperature, < 1 keV. Auxiliary heating allows increased temperature at the expense of density at constant β, or an increase in density towards the density or β limit, if not yet reached.

References:

[1] F. Troyon, R. Gruber, H. Saurenmann, S. Semenzato and S. Succi, Plasma Physics 26A (1983) 209.

[2] A. Sykes et al., Proceedings of European Conference on Plasma Physics and Controlled Fusion, Aachen (1983).

2. TCV PARAMETERS

The essential parameter of TCV is the maximum plasma elongation which must be accommodated in the device. We propose a maximum elongation of 4/1 in a racetrack configuration for the following reasons :

- it is twice the largest elongation studied up to now in a quasi-steady state tokamak;

- equilibrium calculations have shown that above an elongation of 2/1, hollow q profiles can develop even for peaked current profiles due to the elongation of the central flux surfaces. There is no way to predict the degree of peaking of the current profile and it is one of the problems to be studied. In this respect an elongation of 4 can be considered as large and should be sufficient to elucidate this point;

- varying the elongation from 1 to 4 should allow a clear identification of the dependence of the plasma parameters on elongation.

The extensively studied scenario described in this report for obtaining this 4/1 elongation is to start with a circular plasma, with low $q_a \approx 2$, and then to elongate it in a controlled manner. A relatively long plasma pulse, hundreds of msec. with a minor radius a = 18 cm, is planned so as to explore resistive phenomena and current profile diffusion and to allow the plasma to reach quasi-steady state conditions.

The choice of three parameters: toroidal field, minor radius and aspect ratio, fix the size and the characteristics of the machine, shown in Fig. 1.

The toroidal field is chosen to be 1.5 Tesla, the same as in TCA. It is low enough to use our proven demountable coil technology and high enough to give good quality near-circular plasmas.

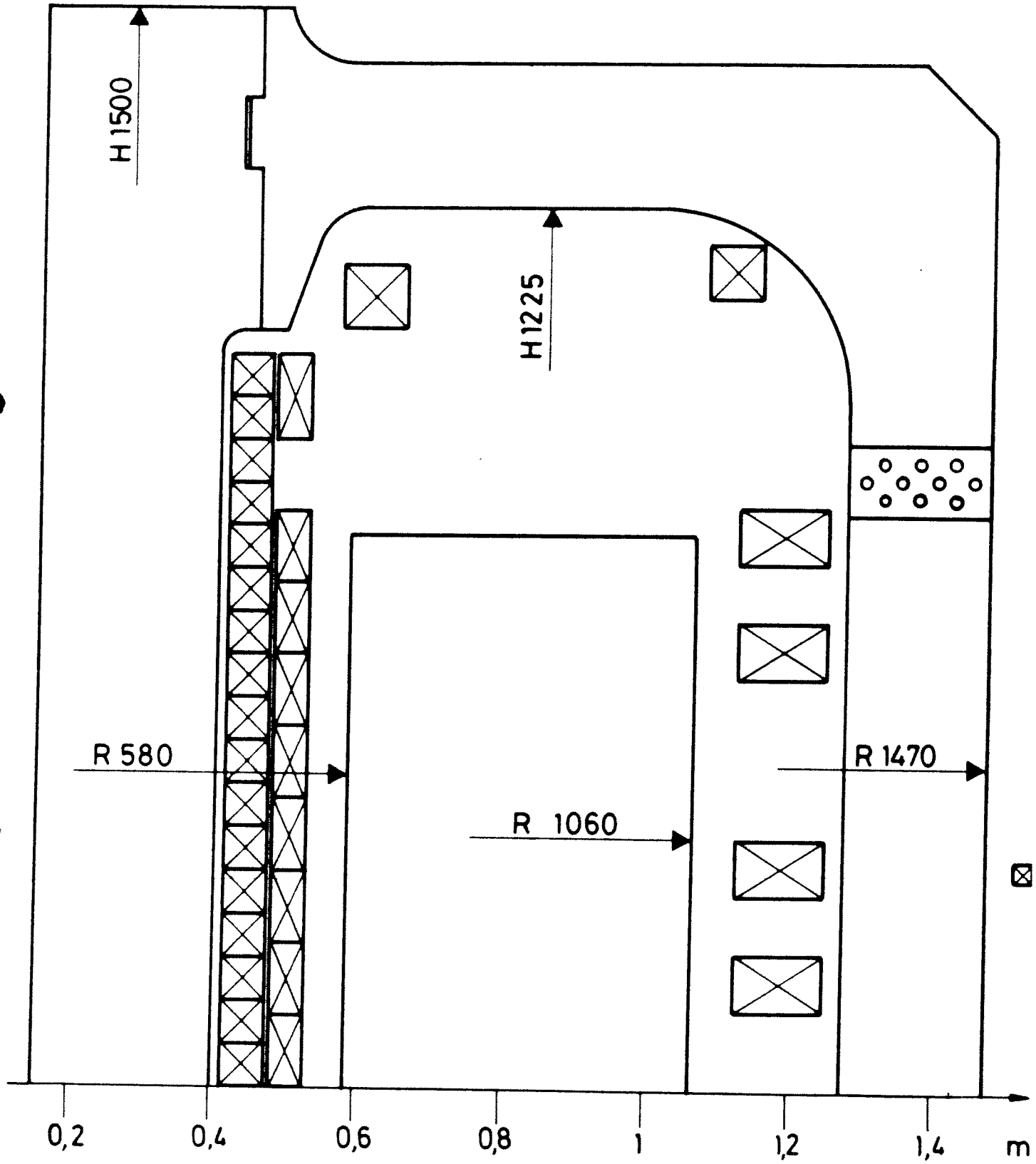

Fig. 1 TCV Reference design

The horizontal minor radius is 0.18 - 0.20 m, the same as in TCA. The plasma minor radius determines the machine size, port access, shaping coil spacing, etc. The resulting coil spacing allows standard diagnostic ports (0.15 m i.d.). A smaller plasma would require an excessively compact construction and also reduce diagnostic access and volt-second capability. A larger plasma would result in too expensive a machine.

A major radius R = 0.8 m leads to an aspect ratio A = 4.0 → 4.4. The major radius is increased from the TCA radius of 0.61 m in order to allow for a large increase in available volt-seconds, up to a swing of -1.2 to +1.2 Volt-sec., with the presently proposed power supplies. This capability provides many options. If it proves possible to produce the maximum 4/1 elongated plasma with q = 2, then 2.4 Volt-sec. provide 1.5 Volt-sec. for the inductive requirement and 0.9 Volt-sec. for both buildup loss and a flat-top current of several hundreds of msec. In TCV, a circular plasma would be obtained with a small fraction of the available volt-seconds. A sufficiently high central electron temperature, ≈ 1 keV, can in principle be maintained in order to keep the resistive losses small during the buildup to high current. The ohmic coil is inside the TF coil (linked) to provide as much space as possible for the transformer flux.

The rectangular vacumm vessel, 0.48 m wide, ± 0.77 m high, allows 0.40 m full-width plasmas with 0.04 m gaps on each side, or 0.36 m full-width plasmas with gaps of 0.04 and 0.08 m to allow for possible auxiliary heating antennae. A gap of 0.04 m → 0.08 m on the sides and at the top is a compromise between good plasma-wall isolation and stabilization from the conducting vessel wall. The box height accommodates plasmas with elongations up to 4/1 of a 0.36 m width plasma, with top/bottom gaps of 0.05 m. If the plasma width is increased to 0.40 m, the maximum elongation becomes 3.6.

The two vertical shaping coil stacks have uniformly spaced coils at small major radius, and 4 groups of 2 at large major radius, allowing 3 large vertical gaps 0.22m high: This arrangement allows good diagnostic access from top, bottom and outside, the same as in

TCA in order to use its diagnostic and vacuum systems, consistent with shaping flexibility and a minimum of total shaping current. For highly elongated plasmas, the sum of the absolute values of the coil currents is less than 1.5 times the plasma current for racetracks. It was found that the shaping coils could be much further away from the vacuum vessel and still produce the same equilibria, with a tolerable increase in total current. The coils are controlled by feedback signals from flux loops and magnetic probe coils on or in the vessel. Each coil is decoupled from the ohmic primary by parallel connection of an equal number of turns. This flexible system avoids the necessity to hard-wire the field shape.

3. MHD EQUILIBRIUM CALCULATIONS

The currents for the coils of the plasma shaping system were calculated by the computer code TCVMHD. This code computes axisymmetric, free-boundary tokamak equilibria with a predetermined plasma shape. Several racetrack equilibria were calculated with elongations ranging from 1/1 to 4/1. In addition, divertor configurations and bean-shaped equilibria can be produced by this coil configuration.

The different design parameters obtained with this code include the power consumption and the Volt-seconds needed for each coil, the sensitivity of the equilibria to the position of the coils and the plasma-wall distance.

4. DYNAMIC MODELLING AND CONTROL

The STARTUP time-dependent resistive MHD-simulation code is used to model the TCA startup sequence, in order to determine the axisymmetric stability and control properties of the device. The code was used at Princeton by Steve Jardin to design the Spheromak and PBX experiments. A positionally stable series of equilibria has been evolved continuously from a circular plasma up to a 4/1 elongated racetrack, using feedback control and vacuum vessel wall stabilization. A

detailed control system design was implemented in these simulations, which uses flux measurements near the vacuum vessel wall to control orthogonal dipole, quadrupole, and vertical field distributions superimposed upon preprogrammed coil currents.

5. PRELIMINARY DESIGN OF THE LOAD ASSEMBLY

Preliminary mechanical, thermal, and electrical design studies have been made for the major systems. The toroidal field coils are roughly rectangular and fully demountable. The central OH solenoid and inner shaping coils are wound directly onto the toroidal coil centrepost. There are 16 shaping coils, each with the same area and number of turns for parallel decoupling connections with the OH coil. A thick-walled vacuum vessel with an insulating gap is being considered, which would have similar diagnostic access as TCA.

The concept would appear to be feasible from a technological point of view, but further optimization will be necessary on all systems.

6. POWER SUPPLIES AND MOTOR GENERATOR REQUIREMENTS - PRELIMINARY ESTIMATES

Each of the major power supply systems has been examined so that preliminary estimates can be made of their specifications and of the power requirements from a motor-generator. An overall efficiency of 75% from motor generator to coil terminals is used for the estimates. The toroidal-field coil system requires the largest amount of energy from the motor generator, 59 MJ with an accompanying peak power of 36 MW. The ohmic system has the highest peak power requirement, 57 MW, and requires 15 MJ of energy. The shaping coils only require an externally supplied 0.4 MJ of inductive energy, some of which could be stored in continuously topped-up capacitors for peak power supply. Coil resistive losses can be made up from the motor generator, requiring 12 MW and 9 MJ. A reserve of 13 MJ and 27 MW is allowed for

auxiliary heating or additional ohmic capability. The estimated minimum requirements for the motor generator are 95.5 MJ of extractable energy, and a peak power of 118.2 MW near the end of the plasma pulse. The peak powers of each system do not occur simultaneously, and therefore the total peak power is less than their sum.

7. DIAGNOSTICS, DATA ACQUISITION, MACHINE CONTROL

Magnetic diagnostics for plasma shape, pressure, current, voltage, position, and fluctuation levels are vital for any non-circular shaping experiment. We will use techniques for measurement and analysis extensively developed on many tokamaks. Many of the diagnostics from TCA can be transferred to TCV. The successful techniques and equipment developed on TCA for data acquisition and machine control can serve as a basis for the TCV systems.

8. PLASMA PARAMETERS AND HEATING

It is obvious that, as yet, no suitable scaling laws for energy confinement, density limits, and beta limits exist for such highly-elongated cross sections. If we were to apply the scaling laws for moderately elongated plasmas, characterized by a very strong scaling with elongation, for the 4/1 elongated plasma in TCV, we would obtain the following values: I_p = 1.7 x 10^6 Amps, $\langle\beta_T\rangle$ = 20%, central T_{eo} = 0.9 keV, τ_E = .440 sec., n_e = 2.2 x 10^{21} m^{-3}!!!! These numbers are most unlikely to be realized, but we do not know at what elongation the scaling laws break down. However, even at an elongation of 2/1, the plasma current, beta, confinement time, and density limit should all increase by a factor of 2.5 at constant limiter q.

Options for auxiliary heating are briefly considered. The high-power AFCO system for variable-frequency wave heating in the Alfvén range (1-5 MHz) (currently being installed on TCA) would be available for the TCV experiment.

9. BUILDINGS, COST, MANPOWER, PLANNING

An estimate is presented of building space requirements and preliminary floor plan for TCV, its systems, and the motor generator. The major system costs are estimated as: SFr. 5 Million for the load assembly: SFr. 6 Million for power supplies; SFr. 6.5 Million for the motor generator. The costs assume the maximum possible transfer of equipment from TCA to TCV. The estimated requirements are 24 professional man-years for design and construction, plus 34 technical man-years for construction, plus technicians from industry to install delivered equipment. The estimated time between Phase II engineering approval and operation is slightly more than 3 1/4 years.

10. BIBLIOGRAPHY

A short discussion of some of the relevant references is presented.

Chapter I. MHD EQUILIBRIUM CALCULATIONS

Section 1 - INTRODUCTION

In this chapter, MHD equilibrium calculations for the presented design for the poloidal field shaping and control system of TCV are described. In section 2 of this chapter, we discuss the code TCVMHD, a physics/engineering programme that uses input which describes a shaping coil and vacuum vessel configuration and a desired plasma shape evolution. It makes an initial guess at shaping coil currents, calculates an MHD equilibrium, does a positional stability test, and plots out vacuum fields and the time evolution of several physics, engineering and control parameters. In section 3, sample equilibria with maximum elongation are shown, in section 4, a sequence of equilibria is described, each of which could be studied separately or used together as a buildup scenario. In section 5, other possibilities of coil connections and coil positions are described. In section 6, bean-shaped equilibria are discussed. In section 7, a sensitivity study is presented which shows the consequences of variations of coil position and shaping on total coil currents, resistive coil power, and plasma volt-second requirements.

Section 2 - CODE TCVMHD DESCRIPTION

The ideal MHD equilibrium code TCVMHD is used to calculate the preprogrammed coil currents for input to the time-dependent STARTUP code. TCVMHD computes axisymmetric, free-boundary tokamak equilibria with a predetermined plasma shape. The calculation proceeds in two steps. The first step provides an initial estimate of the required coil currents by a matrix inversion method. In the second part, these coil currents are used as an initial guess in a free-boundary MHD equilibrium calculation, which solves the Grad-Shafranov equation. The converged solution then gives a plasma shape which very closely approximates the shape that was initially specified.

Each equilibrium is tested for positional stability by adding a small dipole and quadrupole perturbation while freezing the flux on

the wall. Whenever a new converged equilibrium has been found which is very similar to the previous one, this is taken as an indication of positional stability. A detailed calculation of axisymmetric stability is performed by the STARTUP code, described in the following chapter.

In order to generate input data for the STARTUP code, TCVMHD was used to compute several racetrack equilibria (Table I in Chapter II) with elongations ranging from 1/1 to 4/1.

Section 3 - EQUILIBRIUM CONFIGURATIONS

Sample equilibrium configurations are shown in Figs. 1-3. The flux surfaces of the converged free boundary equilibrium are plotted, and the 10th (dotted) surface is the limiter flux surface. The current and pressure radial variation through the plasma midplane are shown above. The current is the broader of the two profiles. In the Figs. 1-3 (b), the results of the positional stability test are shown. The vacuum field is shown in Figs. 1-3 (c). The spacings from the plasma boundary to the vacuum vessel wall are 0.04m on the inside midplane, 0.08 m on the outside midplane, and 0.05 at the top and bottom. The listed values for β_T, q_a, and I_p are used as design plasma parameters.

A different vacuum vessel option is under study, where the vessel is asymmetric with respect to the coils, leaving the vessel top wall near the plasma for stability, but lengthening the lower vessel to allow more space for diverted plasmas. Additional coils could also be added if necessary.

Section 4 - SEQUENCE OF EQUILIBRIA

The key question in shaping experiments is how to proceed from plasma breakdown to the desired final stage. One method is to ramp up all the currents for a given elongation until the final state is reached. However, the plasma would have to maintain a relatively flat

current profile the whole time, to avoid collapse. This may be possible depending on plasma skin time and current rate of rise, but the large, destabilizing decay index of the vertical field may make the experiment very difficult.

The method proposed here and examined extensively might give more control over the plasma during the buildup. The techniques for obtaining $q_a = 2$ at the limiter for a circular plasma are well established. The philosophy of building up the plasma from a circle to the maximum elongation, keeping $q = 2$ at the limiter the whole time, is illustrated in Figs 1-3. Each equilibrium is a separate calculation, but it is possible to pass smoothly from one to another, since the current profiles in the plasmas are relatively flat. This scenario has been verified from 1/1 to 4/1 by the resistive MHD code STARTUP (see next chapter). In Fig. 1, the 1/1 plasma is centred at the upper diagnostic port. At higher elongation, the upper plasma is within 0.05 m of the top of the vessel, which now contributes as fully as possible to the positional stability of the plasma. To maintain this distance, the magnetic axis of the plasma moves down. One of the key features to be studied in the experiment will be the effect of the plasma-wall distance. In the following figures, the parameters relating to 8 successive equilibria are summarized. In this case the time scale is chosen to give an approximately linear rate of rise of the plasma current, followed by a flat top when β_T is increased, to simulate the behaviour of a 1.0 sec. long plasma discharge.

In Figure 4, the plasma current and the inductive volt-seconds required from the ohmic transformer coil are shown. In Fig. 5 the single turn current (kA), inductive volt-seconds, and resistive voltage (V) for a representative coil are shown. For this macrocoil (two or more coils), the values are at the terminals of the coils in series, e.g. for two turns. For this sample, the R and Z of the coil centre and the area and the copper fraction of the first coil in each group are shown. To obtain the terminal voltage, the inductive voltage can be found from the derivative of the inductive volt-seconds, and added to the resistive volts. The power supply requirements on voltage and current are thereby specified, when normalized to the actual number of turns.

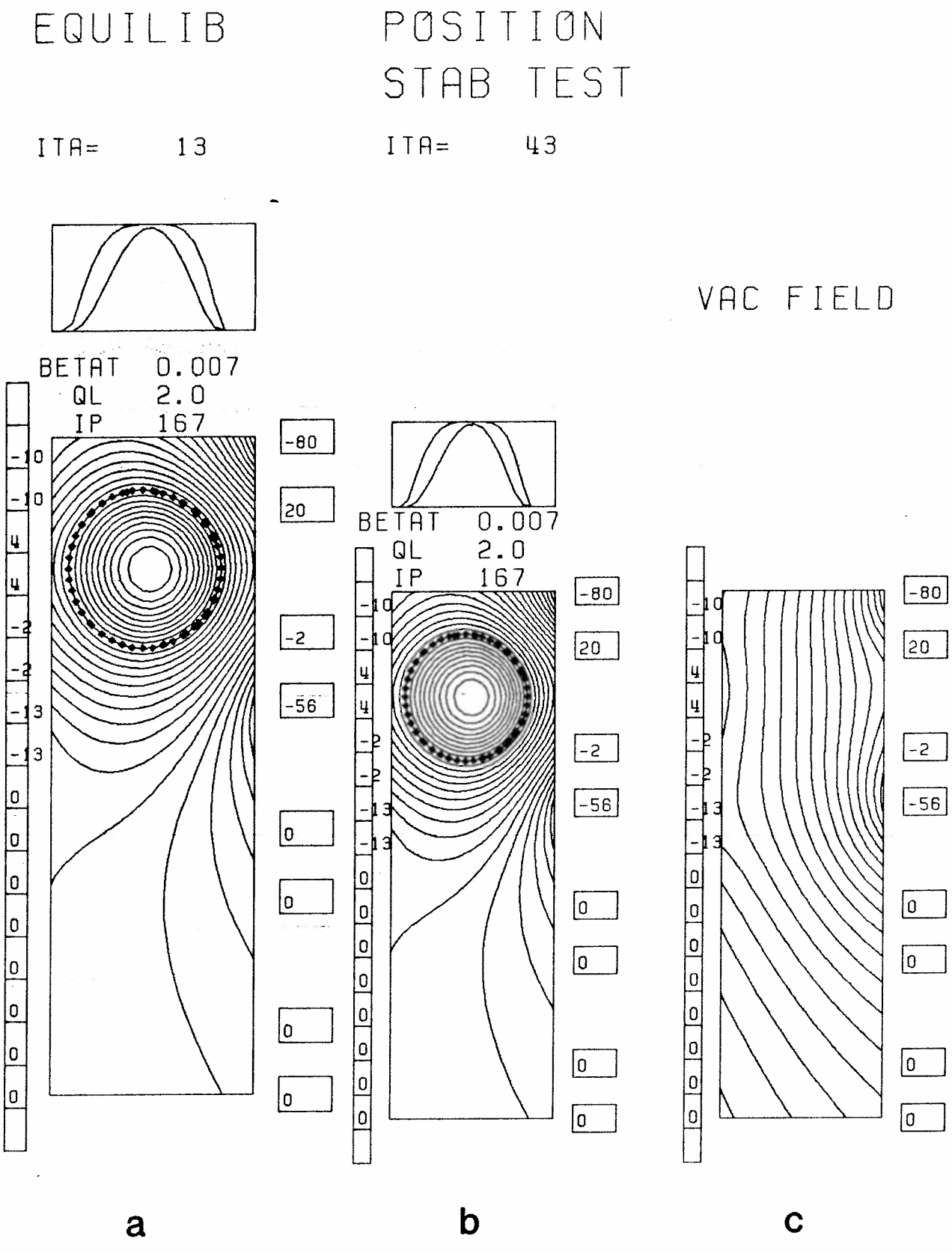

Fig. 1 K = 1 circle

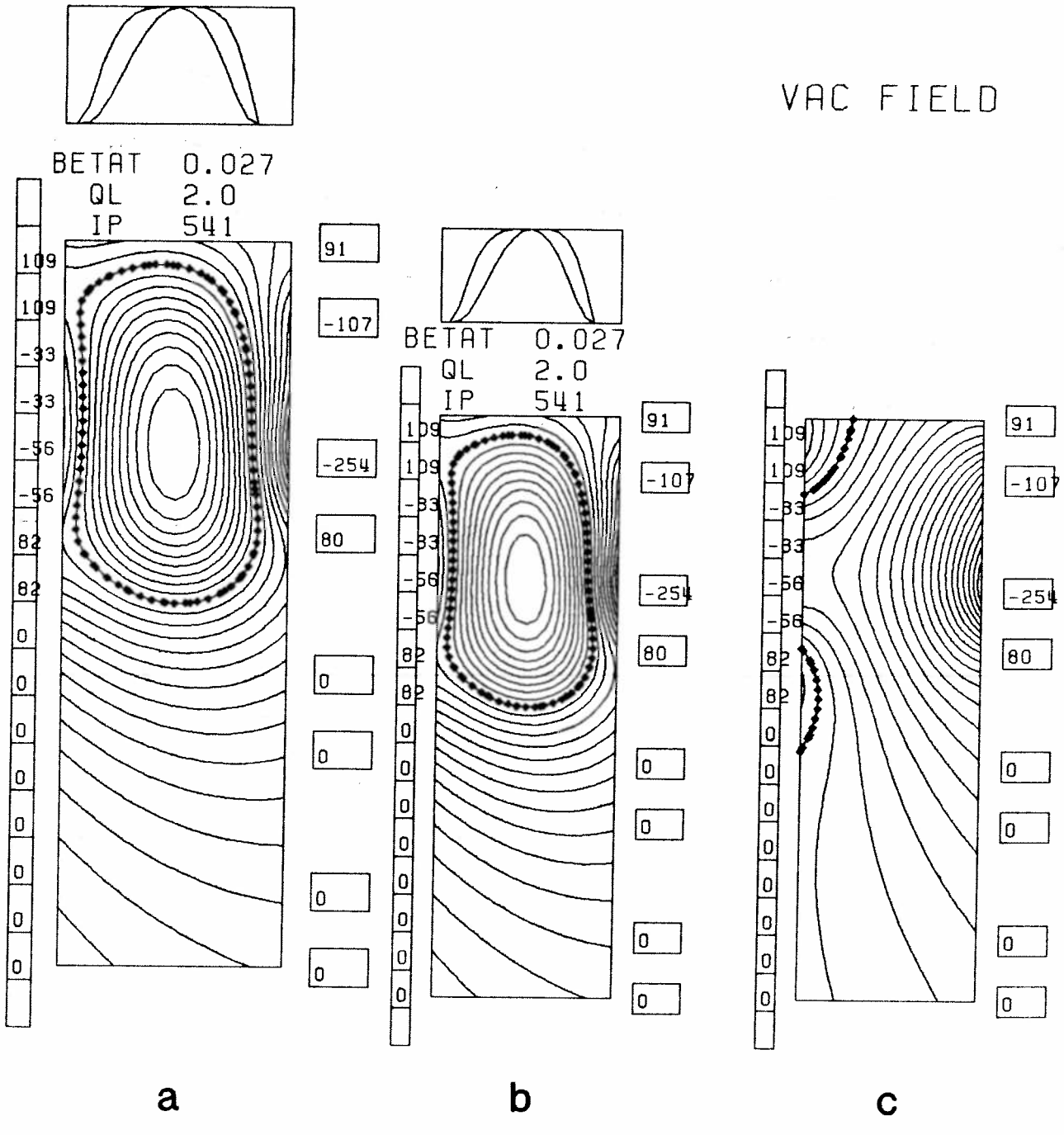
EQUILIB
POSITION
STAB TEST
ITA= 18
ITA= 54
VAC FIELD
BETAT 0.027
QL 2.0
IP 541
BETAT 0.027
QL 2.0
IP 541
a
b
c

Fig.2 K = 2/1

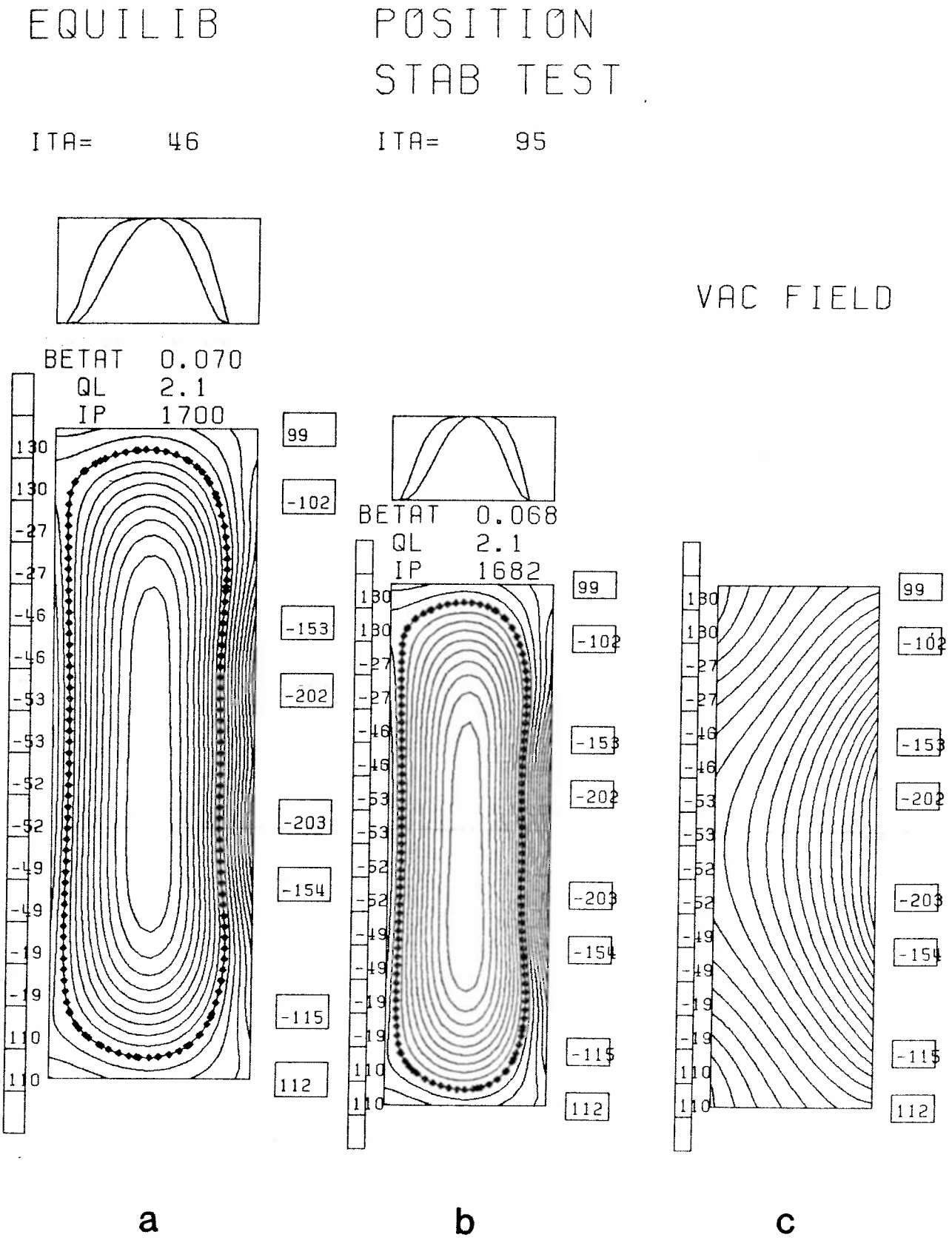
EQUILIB
POSITION
STAB TEST
ITA= 46
ITA= 95
VAC FIELD
BETAT 0.070
QL 2.1
IP 1700
BETAT 0.068
QL 2.1
IP 1682
99
-102
-153
-202
-203
-154
-115
112
a
b
c

Fig. 3 K = 4/1

In Figure 6(a-d), several shaping coil and MHD equilibrium parameters are summarized. The parameters are listed from top to bottom in Table 4. The notable features of these graphs are summarized: At the full plasma current, Fig. 6a2 shows that the ratio of coil to plasma current is negative, contributing volt-seconds to the plasma. In Figure 6a3, the ratio of absolute coil to plasma current is only about 1.3/1, which is acceptably small at full current. In Figure 6b, the limiter q_a = 2 is constant. The near central q (which starts near 1.0) increases at high elongation to above 2, due to the highly elongated central flux surface, leading to a nonmonotonic q-profile. The implications of this for stability, for sawteeth and plasma current resistive peaking remain to be investigated. In Figure 6c, the toroidal beta increases monotonically. In Figure 6d, the elongation increases roughly linearly with time, as the Z axis moves downward. The major radius of the magnetic axis is nearly stationary.

Section 5 - ALTERNATIVE COIL CONNECTIONS

In Figure 7, with a different coil set, the coils are connected so that there are only 8 macrocoils instead of 16. Pairs of coils are connected in series to cut the number of coils in half. The vertical spacing of the outer coils was uniform. With fewer coils to control the shape, the plasma has a dee-shape with similarities to an expanded-boundary single null divertor configuration. (In these plasmas, the shaping currents are all negative, so fewer external volt-seconds are required.)

Section 6 - "BEAN"-SHAPED PLASMAS

The plasma-shaping coils in TCV are designed and optimized to produce racetrack-shaped plasmas, while allowing good diagnostic access. However, the flexibility of the system allows a very wide range of plasma shapes, since there are enough coils to produce a highly variable flux distribution on the two walls of the box.

TABLE 4

Parameters in Figure 6

Letter	Number	Explanation
a	1	Total resistive power in shaping coils (watts)
a	2	Ratio of the sum of currents in the shaping coils to the plasma current
a	3	Ratio of the sum of the absolute value of currents in the shaping coils to the plasma current
b	1	Safety factor q on the flux surface near the axis, at 90% (Flux axis - Flux boundary)
b	2	Safety factor q at limiter
b	3	Maximum plasma current density (kA/m^2)
c	1	Plasma volume-averaged toroidal-beta at B_T = 1.5 T
c	2	Plasma poloidal β_I
c	3	Maximum plasma pressure (MKS) ($10^5 \approx$ 1 Atm)
d	1	Height to width ratio (elongation) of plasma boundary surface
d	2	Z-position of magnetic axis in equilibrium (Note: internal x-points can cause two axes)
d	3	R-position of magnetic axis in equilibrium (Note: internal x-points can cause two axes)

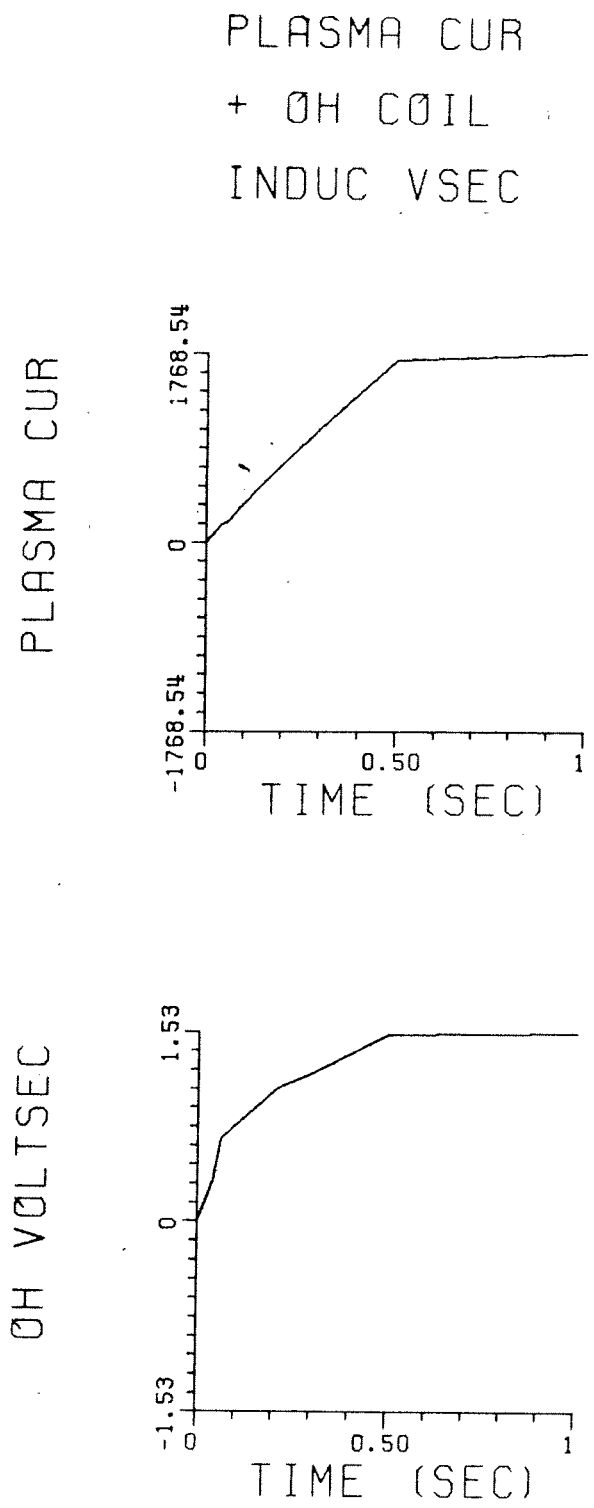

Fig. 4 Volt-seconds (inductive) and Plasma current

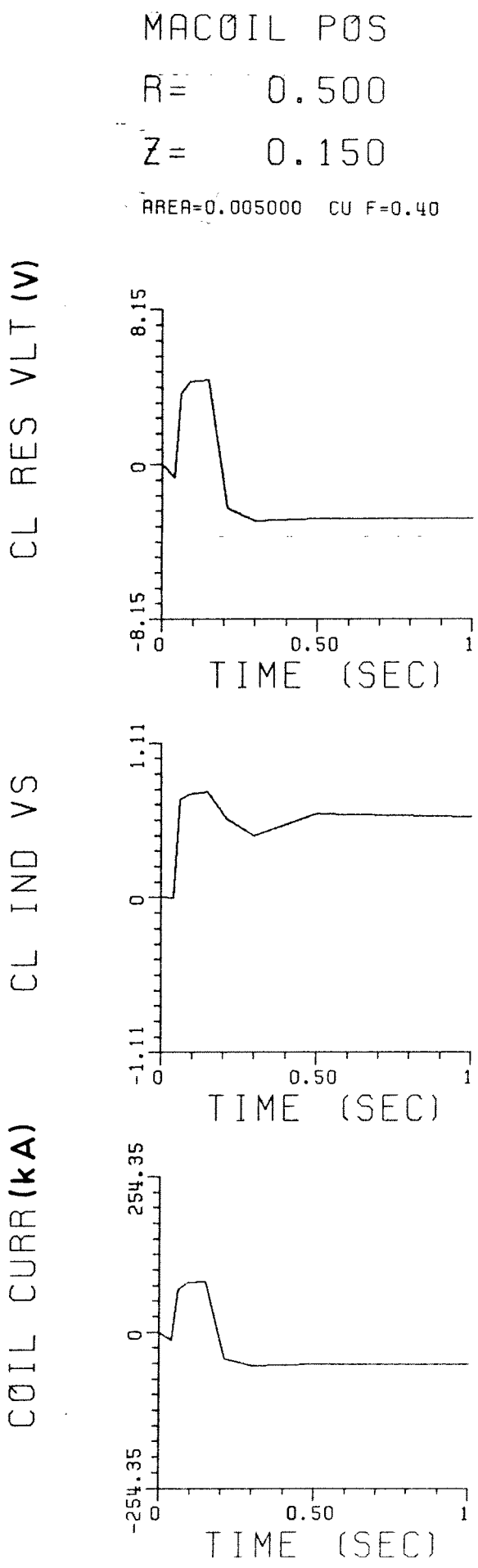

Fig. 5 Time-dependent parameters of shaping coils

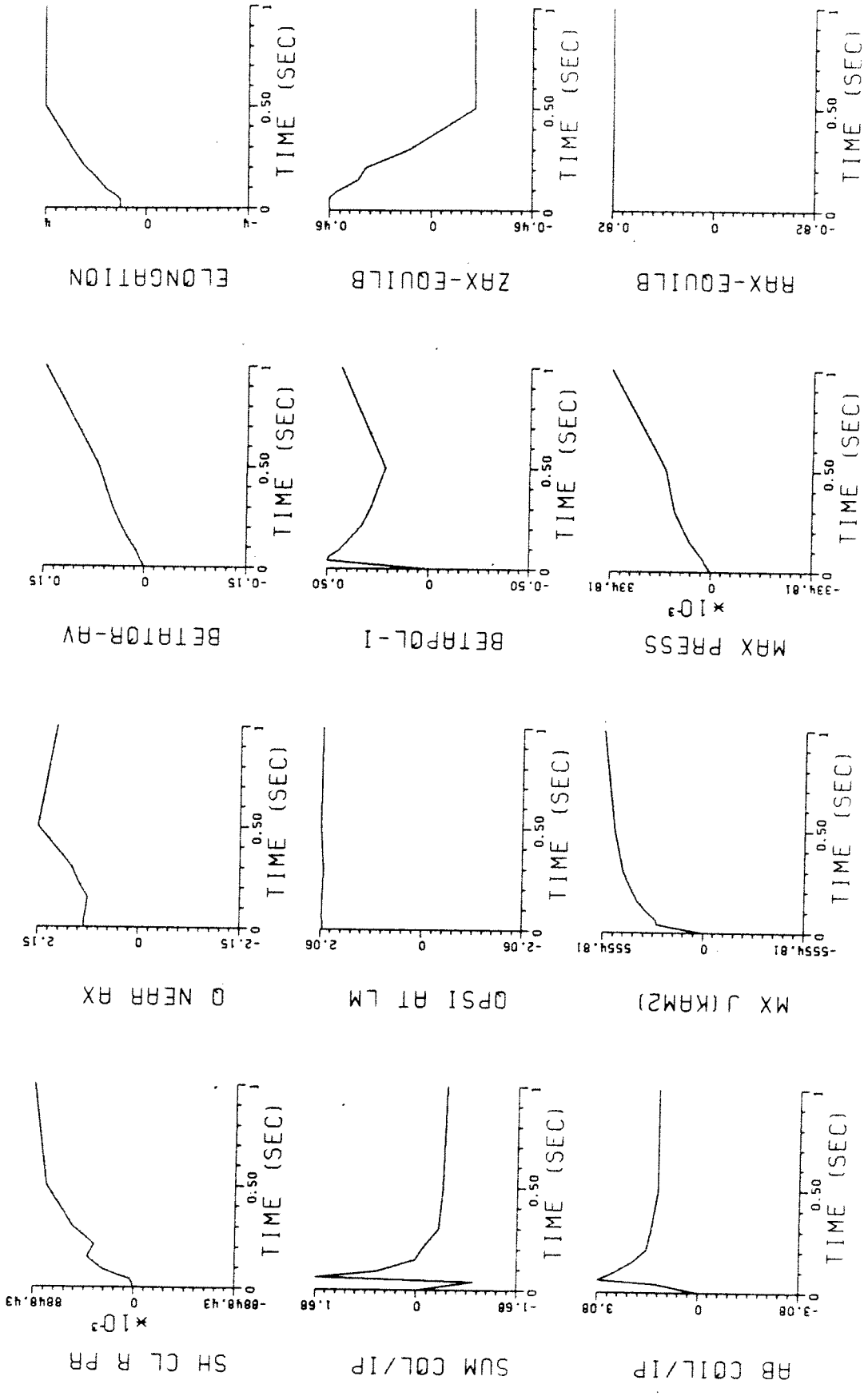

Fig. 6 Time-dependent equilibrium parameters

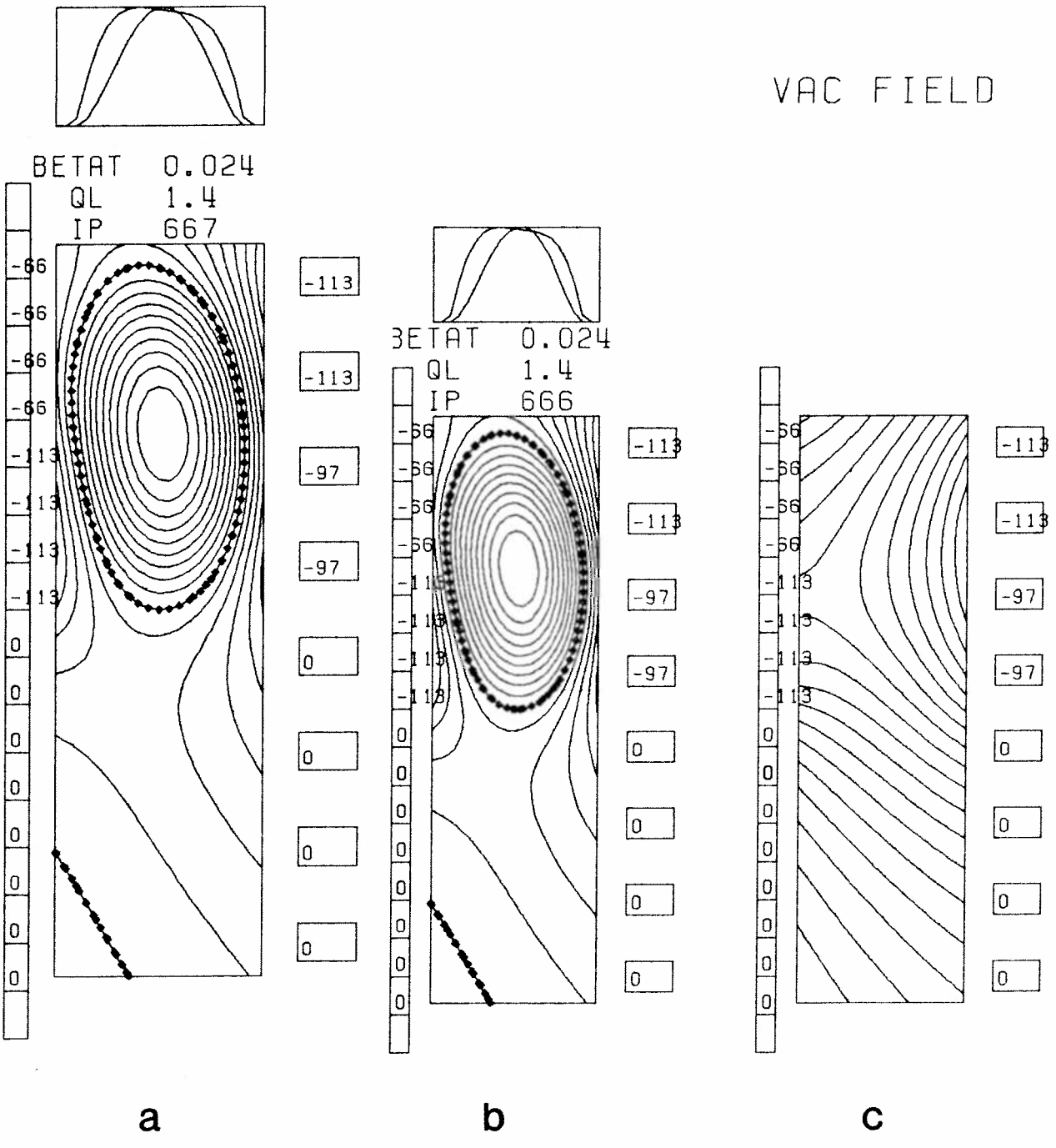

Fig. 7 K = 2/1, 4 macrocoils

We have not attempted to study equilibria of moderate elongation because of the probable need for coils inside the TCV vessel. However, as is seen in Fig. 8, the TCV coil set is capable of producing bean shaped plasmas. The current profile is broad, but still monotonically increasing from zero on the edge to the maximum on axis. In Fig. 8, the plasma is 0.04 m from the outer wall, 0.28 m wide at the midplane, and has a total height of 1.10 m. The X-points are ≈0.05 m from the inner wall. The maximum plasma current is limited by the maximum coil current in the inner stack, in the range (130-150) x 2 kiloamps per macrocoil. Thus it may be possible to study highly elongated bean plasmas with divertors in TCV and compare them with racetracks. However, the positional stability of these equilibria is not known. Beans require approximately 50% more volt-seconds/megamp than racetracks. In Fig. 8, 1.18 inductive volt-seconds are required from the ohmic transformer to produce the plasma, $(\Sigma |I_c|)/I_p=2.7$ and $(\Sigma I_c)/I_p=.08$. The large positive currents near the tips are the cause of the high coil current, and low shaping-coil volt-second contribution.

Details of the buildup trajectory and optimum position and shape remain to be studied. However, it is encouraging that bean equilibria can be found, which may have shapes near the optimum for high beta. The most probable buildup trajectory would be successively elongated racetracks with or without divertor, up to a similar elongation, then push with midplane coils and pull with end coils to obtain the desired shape of the bean.

Section 7 - COIL POSITION SENSITIVITY

In this section, the sensitivity of shaping currents with respect to variations in coil spacing is shown. In Fig. 9, for a 4/1 elongation plasma, four quantities are plotted as a function of the major radius of the outer coil stack, with other parameters being held constant. The four quantities are: the ratio of the sum of coil currents to plasma current; ratio of the sum of absolute values of the coil currents to plasma current, the total resistive coil power, and required volt seconds. It is seen that the variation is small, so there is considerable flexibility for the coil positions. In other

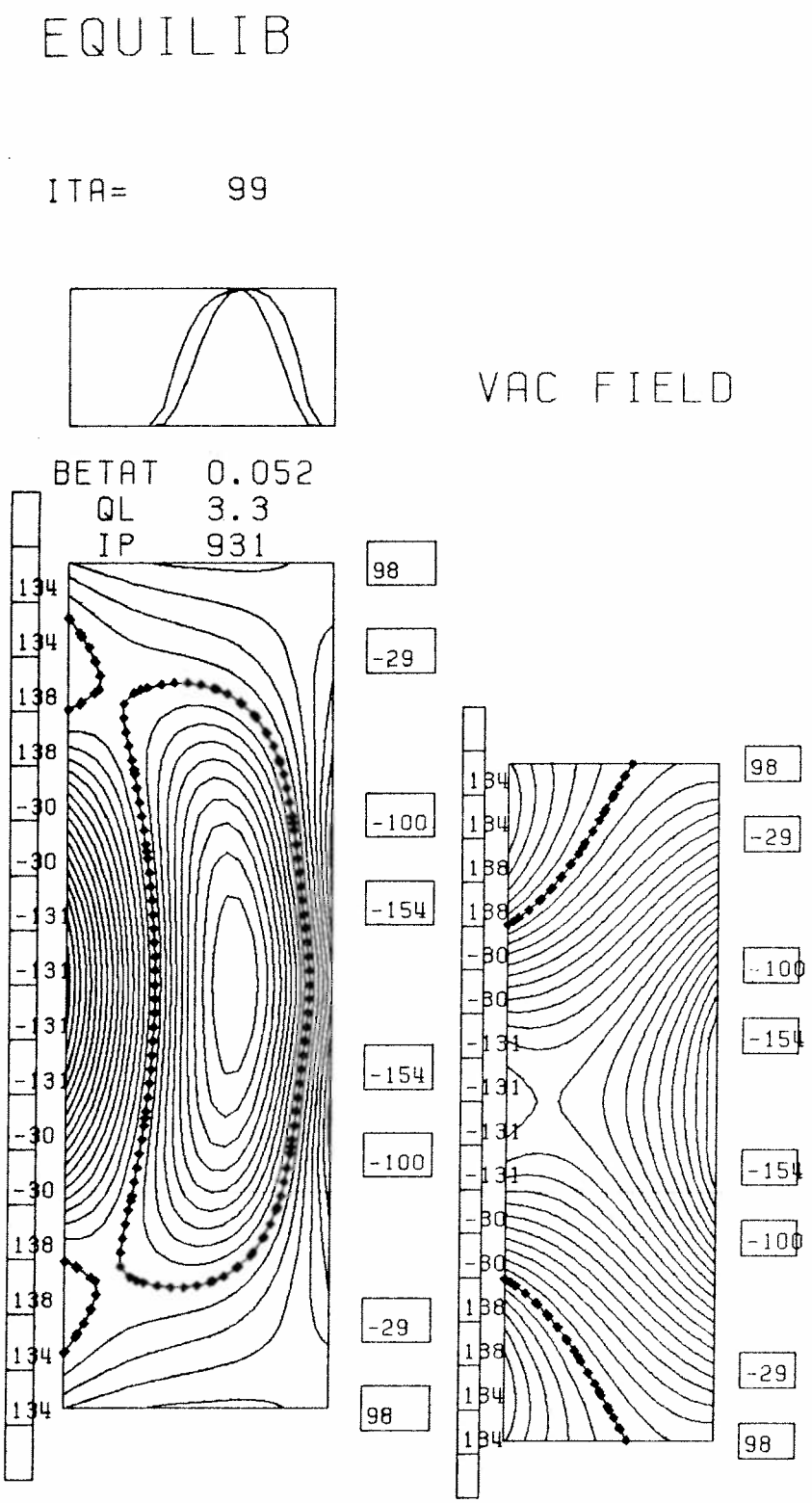

Fig. 8 Bean, Diverted, outer gap = 0.04 m

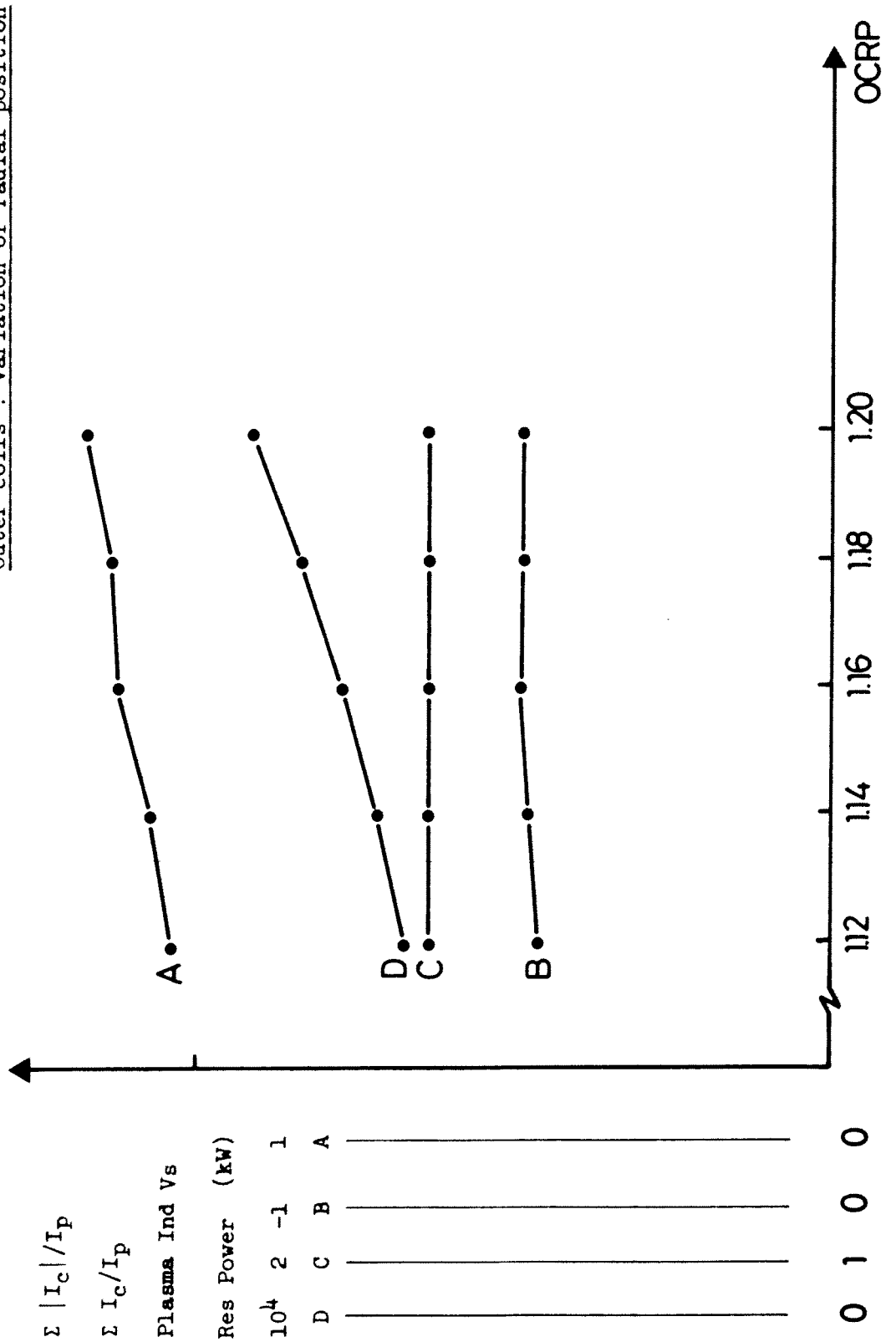

Fig. 9 4/1 plasma variations

studies, the vertical spacing is varied at fixed major radius. In this case the variations are more marked, but still acceptable.

Encouraged by these results, we have studied the effects of increasing the coil to vessel gap to 0.20m, shown in Fig. 10. The equilibrium appears to be very similar to those obtained with near coils, and the walls are still close to aid stability. (Stability tests were not tried with these plasmas.) This spacing is not possible for R = 0.80m in TCV. The current in the remote coils is much larger, but it is still possible to obtain good plasma shaping. A detailed sensitivity to the coil spacing is shown in Fig.11, where the solid and dashed line corresponds to different vertical coil separation of the outside coils.

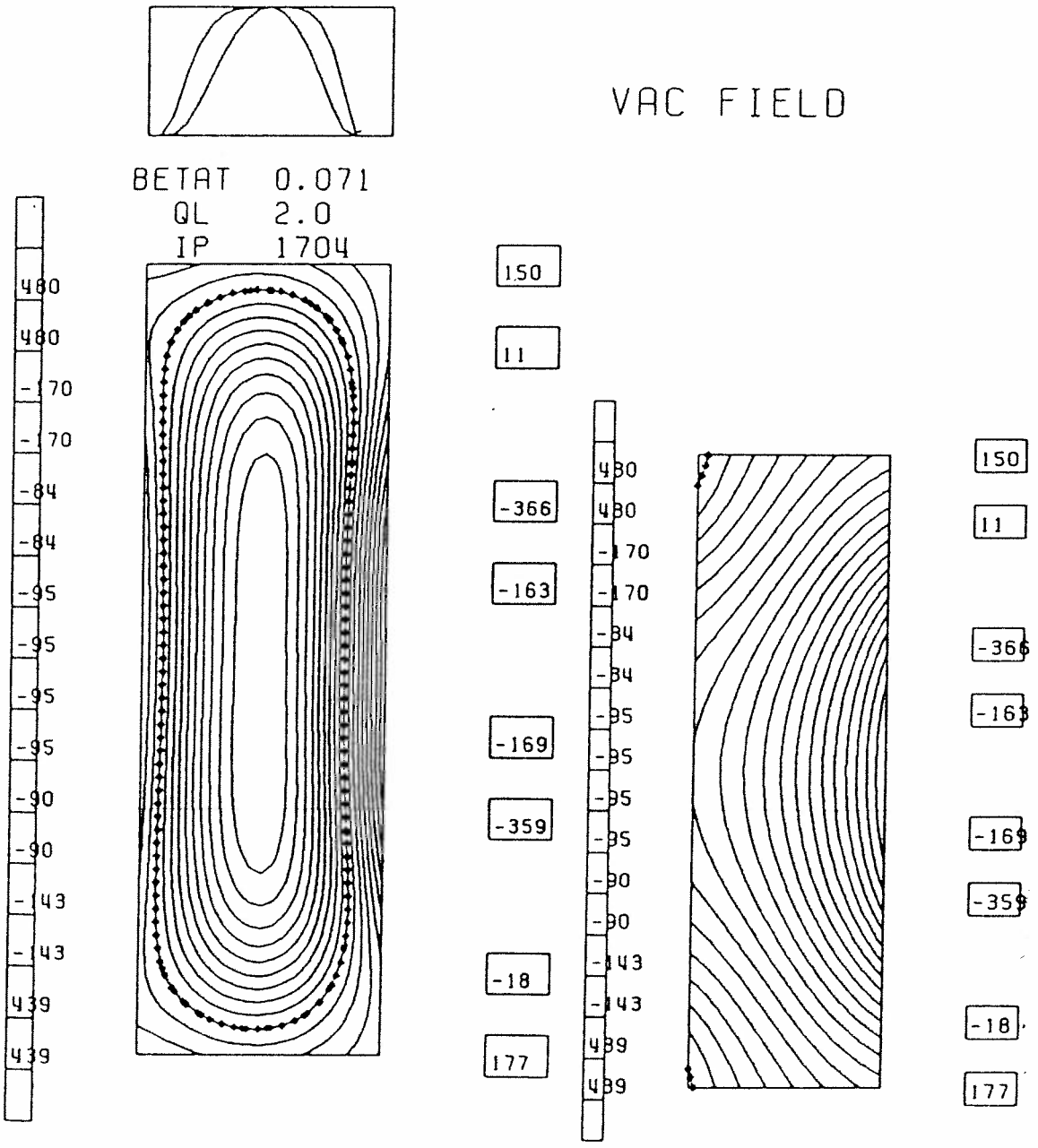

Fig. 10 K=4/1, Remote Coils

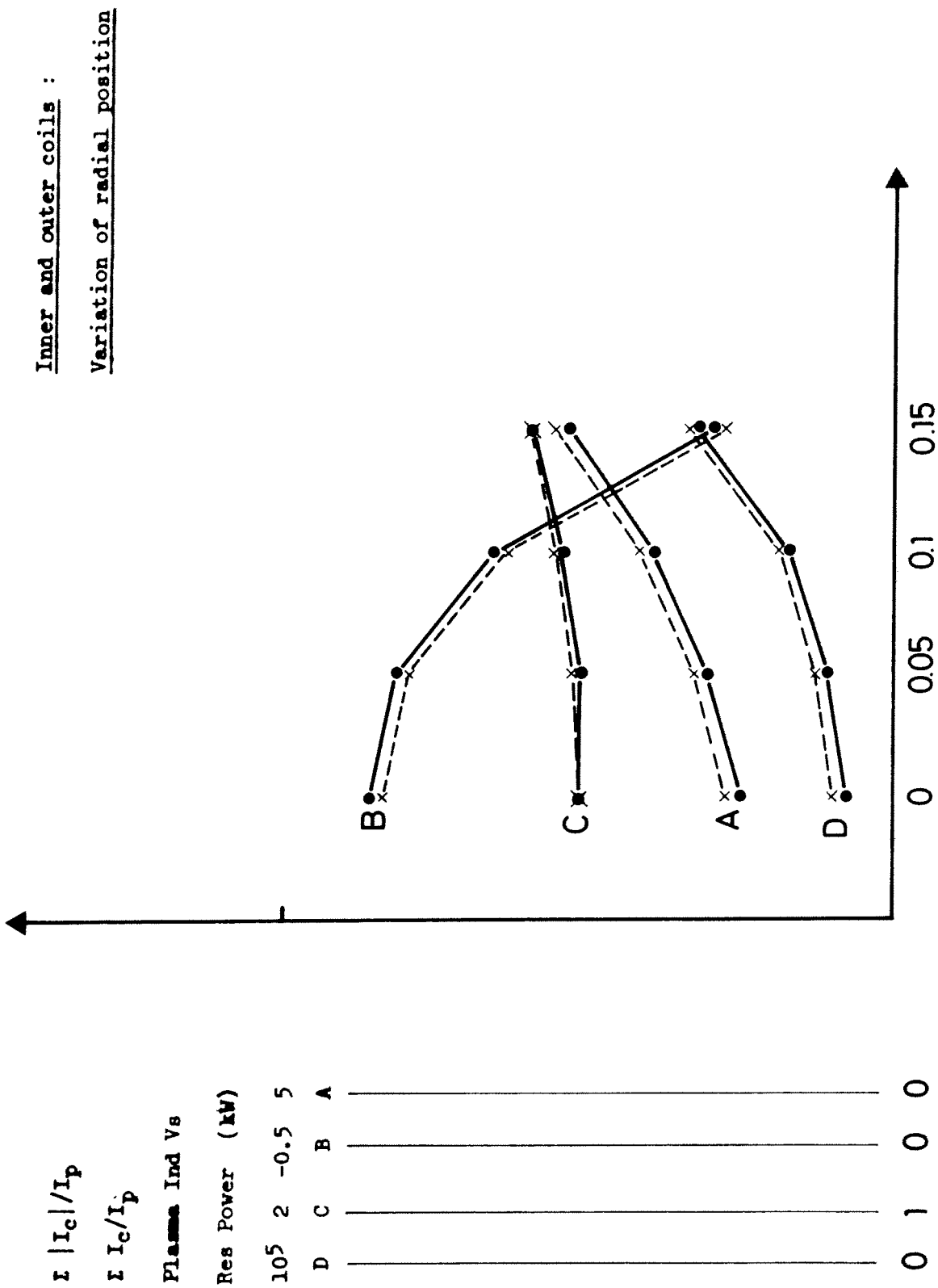

Fig. 11 4/1 Plasma, Remote Coil Variations

Chapter II. DYNAMIC MODELING AND CONTROL : PPPL RESISTIVE MHD CODE

Section 1 - INTRODUCTION

In this chapter we describe studies being carried out with the time-dependent resistive MHD simulation code STARTUP developed at PPL. This code is used to model the current buildup phase and to determine the axisymmetric stability and control properties of the device.

The STARTUP code is a free boundary axisymmetric simulation code which models the resistive time-scale evolution of a toroidal plasma, (Fig. 1) based on the currents supplied by TCVMHD (Table I), including its interaction with the poloidal field coils and other nearby conductors. Circuit equations for the Ohmic heating, equilibrium field, and other poloidal field systems are solved simultaneously with the plasma equations, allowing modeling of passive and active feedback systems for radial and vertical position control. The torus is assumed to have an insulating gap.

Since the STARTUP code is intended to follow the plasma evolution on the resistive time scale, an artificially high mass density and viscosity are used for computational efficiency. It has been verified that these artificially large parameters do not affect the motion of the plasma on the L/R time scale of the passive coil circuits, when realistic values of resistivity and inductance are used.

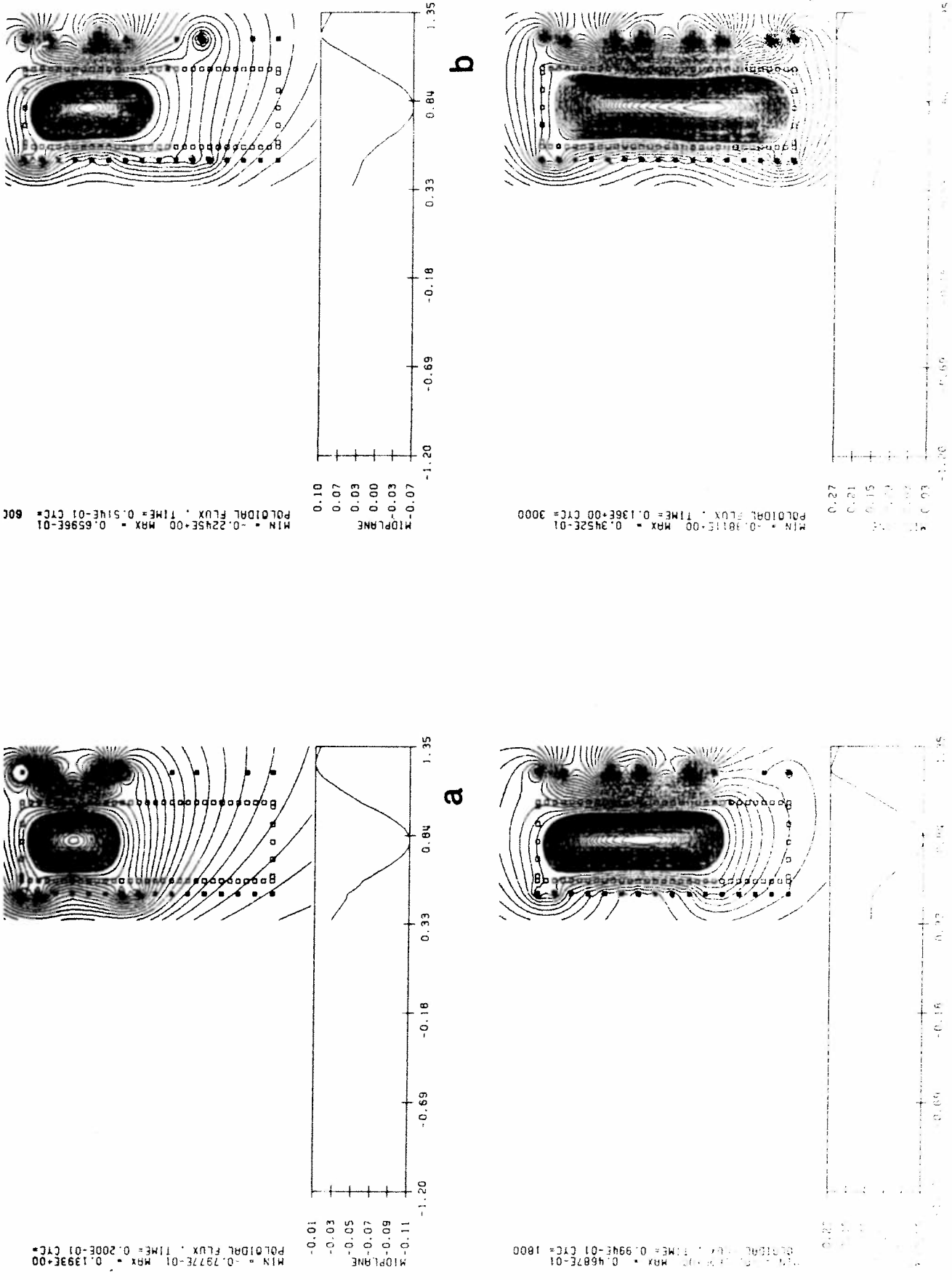

Fig. 1 Evolution of TCV Plasma with Resistive MHD Axisymmetric STARTUP Code

TABLE I. Preprogrammed currents (kA) in each of the 16 EF coils, plasma current and elongation at 8 reference times. Linear interpolation is used to define currents at intermediate times.

	t_1	t_2	t_3	t_4	t_5	t_6	t_7	t_8
I_1	162	164	39	-86	-110	-134	-133	-104
I_2	0	-112	-78	-80	-106	-127	-119	-96
I_3	-40	-66	-53	-58	-60	-71	-68	-48
I_4	174	218	232	224	228	199	220	240
I_5	123	91	79	71	96	99	96	105
I_6	-148	-107	-88	-93	-101	-94	-103	-108
I_7	-140	-254	-198	-153	-151	-167	-168	-154
I_8	88	80	-41	-173	-207	-174	-198	-203
I_9	0	0	-9	-4	-166	-251	-234	-203
I_{10}	0	0	65	74	90	72	-58	-154
I_{11}	0	0	0	0	0	0	-61	-108
I_{12}	0	0	0	0	0	0	132	105
I_{13}	0	0	0	0	0	0	133	240
I_{14}	0	0	0	0	0	0	-28	-48
I_{15}	0	0	131	54	176	72	-39	-96
I_{16}	0	0	49	140	-78	-131	-127.4	-104
I_p	332	541	584	763	1069	1174	1425	1700
K	1.6	2.0	2.25	2.5	3.0	3.25	3.62	4.0

TABLE II. Z-position of control flux loops used at 8 reference times. At intermediate times, control flux is interpolated using loop positions in table, at R = 0.62 m and R = 0.98 m.

Loop #	t_1	t_2	t_3	t_4	t_5	t_6	t_7	t_8
2 and 3	.513	.440	.480	.500	.550	.560	.560	.560
1 and 4	.430	.360	.315	.250	.180	.135	.070	.000
5 and 6	.353	.280	.150	.000	-.19	-.29	-.42	-.56

Section 2 - SHAPING CONTROL FEEDBACK SYSTEM

In this section, we discuss the control system used to maintain plasma position and shape in the STARTUP code. It is recognized that there are a very large number of possible control schemes. Here we present one scheme that works in the simulation. The actual TCV control system will be flexible enough to try this scheme as well as any others. One feature is that here the flux is specified on the desired plasma surface, whereas in the experiment, the flux is measured with flux loops at the vacuum vessel wall, along with the spatial derivative of the flux with a magnetic pick-up loop. These measurements are then extrapolated a few cm to the position of the desired plasma surface.

Active stabilization and control is provided by 4 independent feedback systems for radial field (RF), vertical field (VF), quadrupole field (QF) and plasma current (OH). The first 3 of these systems feedback on sums and differences of the flux measurements on the flux loop 1 to 6 described in Figure 2 and Table 2, while the OH system senses the total plasma current with a Rogowski loop measurement. The loops in Fig. 2 at R = 0.62 and R = 0.98 m are shown at one reference time. As the plasma elongates, different groups of 6 loops are used, and different distributions of feedback currents are used.

A given flux measurement at a given time is in general taken to be an interpolated signal from 2 flux loops.

The state vector for the active subset of flux loop measurements is denoted by

$$\Phi(t) = \left(\Psi_1(t)\ \Psi_2(t)\ \Psi_3(t)\ \ldots\ \Psi_6(t)\right). \qquad (1)$$

The orthogonal vectors corresponding to the 4 control systems and the selected flux loop positions are

$$\begin{aligned} \Phi_{RF} &= (\ 0,+1,+1,\ 0,-1,-1) \\ \Phi_{VF} &= (-1,-1,+1,+1,+1,-1) \\ \Phi_{QF} &= (-2,+1,+1,-2,+1,+1) \\ \Phi_{OH} &= (+1,+1,+1,+1,+1,+1) \end{aligned} \qquad (2)$$

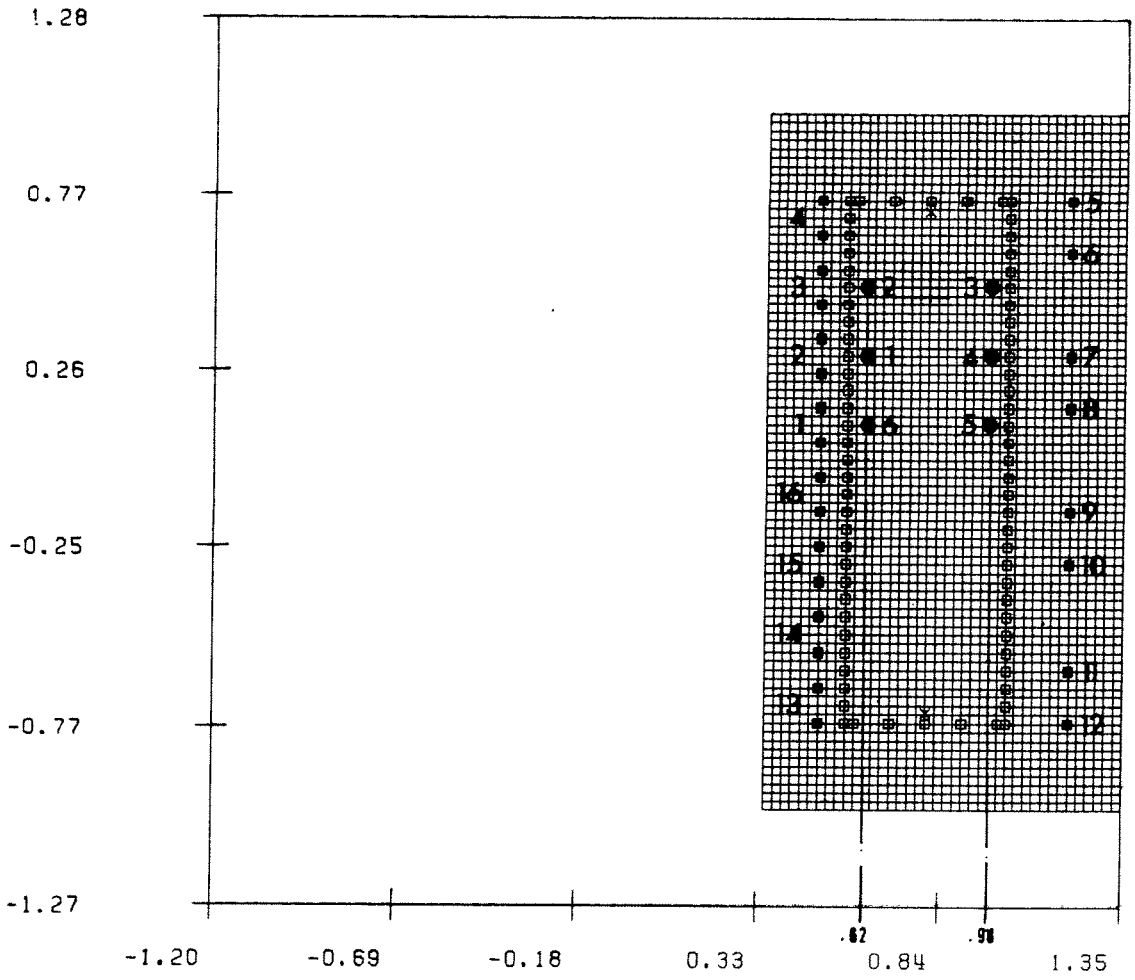

Fig. 2 Coil, Vessel, and Flux Loop Geometry

Corresponding to each of the orthogonal flux measurement vectors of equation (1) is a vector of current amplitudes I(t)

$$I(t) = \left(I_1(t),\ I_2(t),\ I_3(t),\ I_4(t),\ I_5(t),\ I_6(t)\right) \qquad (3)$$

The current vectors for each of the first 3 control systems are determined by selecting 6 coils or groups of coils near the control flux loops, both groups of which are different at each of the 8 reference times. The inductance matrix M(t) between these coil groups and the control flux loops is inverted to obtain the control current vectors at each of the 8 times

$$\begin{aligned} I_{RF}(t) &= M^{-1}(t) \cdot \Phi_{RF}(t) \\ I_{VF}(t) &= M^{-1}(t) \cdot \Phi_{VF}(t) \\ I_{QF}(t) &= M^{-1}(t) \cdot \Phi_{QF}(t) \end{aligned} \qquad (4)$$

Control current vectors at intermediate times are again defined by linear interpolation. For the plasma current control, a "perfect" OH system is modeled in which the poloidal flux everywhere on the computational boundary is increased at the same rate to keep the plasma current on its preprogrammed trajectory.

We are in the process of exploring several combinations of control systems. For the particular example shown in Fig. 1, an extra control system was used to set the flux at the sides equal to the flux at the top limiter point. Other cases have been run successfully with the dipole and quadrupole fields as described here, with plasma current feedback used for radial position control.

In the absence of plasma or additional conductors, the control systems described above are independent in the sense that the flux vector from one current vector is orthogonal to the other flux vectors. This orthogonality property is approximately preserved in the presence of conductors and plasma due to the symmetrical placement of the coils and flux loops. Thus the feedback control voltage for each of the feedback current groups is chosen proportional to the inner product of its flux vector and the flux state vector. These voltages are superimposed on each of the 16 equilibrium field coils, together with the voltages required to keep them on their preprogrammed trajectories.

Section 3 - COMPUTATIONAL RESULTS

The preprogrammed currents determined by the TCVMHD code in each of the 16 independent poloidal field coils are given in Table I, for the coils in Fig. 2. We specify the currents at 8 time points and linearly interpolate to define the currents at intermediate times. Similarly, the dipole and quadrupole feedback systems are prescribed.

The computation is initialized in the equilibrium configuration of figure 1, corresponding to time t_1 in Tables I. A vacuum vessel is modeled as 72 discrete conductors in parallel with each other in series with an insulating gap, each with a resistivity of 0.01 R ohms, where R is the major radius (distance from the symmetry axis). A model ohmic heating system is used to keep the plasma current on the trajectory specified in Table I.

The plasma is shown to evolve in a stable manner up to 4/1 elongation. Examination of the currents required in the feedback systems shows that a maximum feedback current of 20 kA was required to maintain positional control of the plasma during the evolution. The time constant for response of the feedback system is the same as that for the vacuum vessel, of the order of 5 milliseconds.

The plasma elongation in figure 1d is approximately 4/1. The plasma has been stably evolved up to the maximum elongation of 4/1, with positional stability found during the entire evolution.

Section 4 - CONCLUSION

In conclusion, we have investigated a plasma control system which allows the plasma to be stably evolved from a near-circular plasma to a 4/1 plasma. Positional stability is obtained at all times for ideal and resistive axisymmetric modes. The plasma position is sensed at points near the vacuum vessel wall, where flux loops and magnetic field probes can be used to extrapolate to the flux at the plasma surface. Control currents are all superposed on a preprogrammed shaping current distribution.

Chapter III. TCV - PRELIMINARY DESIGN OF THE LOAD ASSEMBLY

Section 1 - INTRODUCTION

The preliminary design presented here is based on proven technology (ISX, D-III, TCA, COMPASS). The following basic design choices were made :

a) The toroidal field coils have roughly rectangular shape. They are constructed of copper plates and are fully demountable.

b) The inner vertical sections of the toroidal field coils are wedged for $R < 0.4$ m.

c) There are two butt joints and two lap joints per turn, as shown in Fig. 1.

d) The OH transformer is located inside the toroidal field coil.

e) The central solenoid of the OH transformer and the inner shaping coils are wound directly onto the toroidal field coil centerpost and the whole assembly is either vacuum impregnated or cured in place.

f) There are 16 shaping coils, each of which has the same number of turns as the OH transformer sections.

g) Each shaping coil is connected in parallel with a section of the OH transformer in order to cancel out the induced voltage.

Section 2 - TOROIDAL FIELD COILS

There are 16 toroidal field coils of 6 turns each. They are constructed of copper plates 23.5 mm thick. The insulation thickness is 1.5 mm between turns and 8.5 mm between coils. A maximum toroidal field of 1.5 T at R=0.8 m is assumed. Dimensions are given in Fig. 1. Bending moments and stresses produced by in-plane magnetic forces have been computed, using the beam model (INT 86/77). The results (Fig. 2) indicate that the design is probably feasible if one uses a high-strength copper alloy, e.g. Cu/Cr, which was used in ISX. This alloy

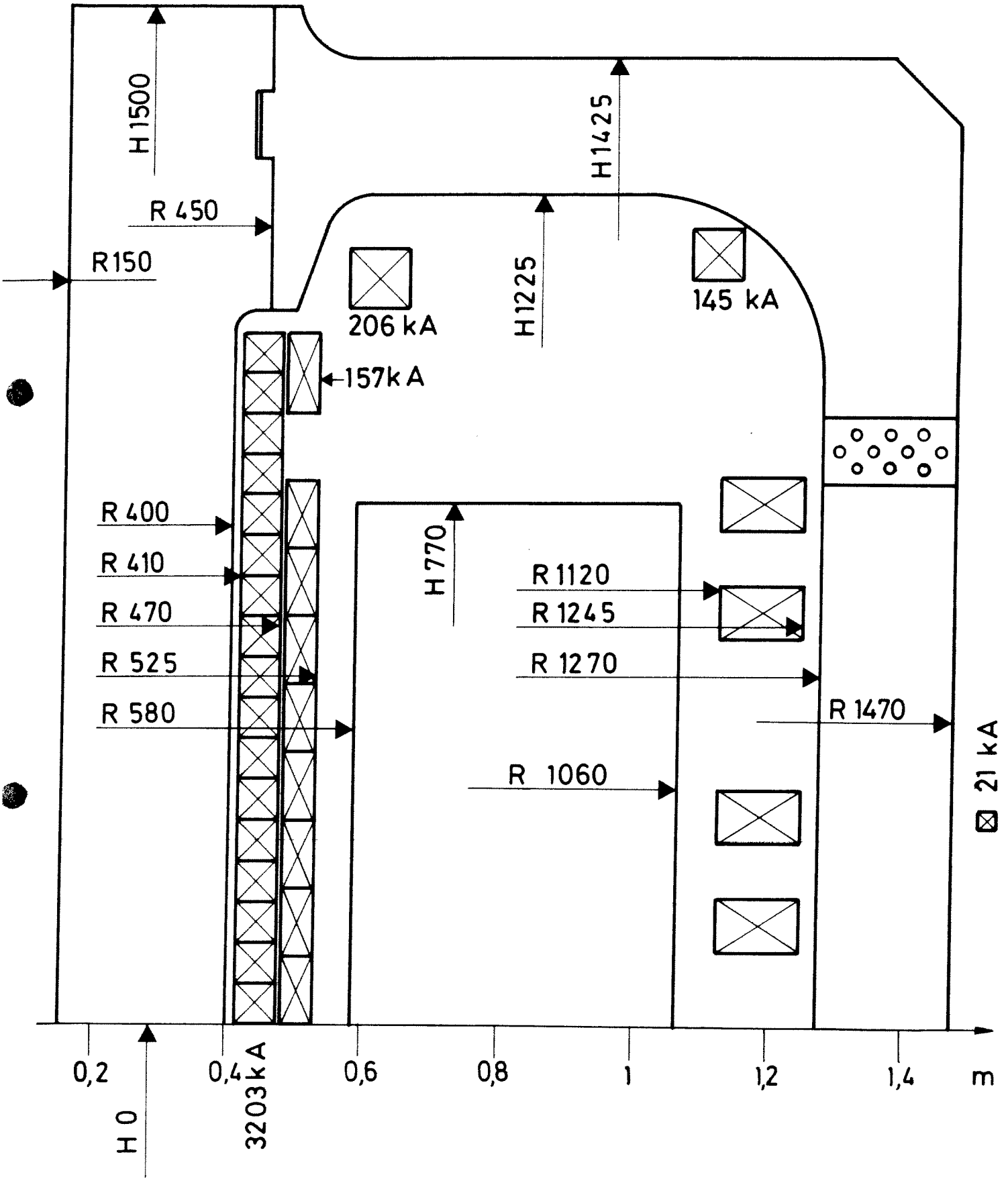

FIG. 1 : TCV REFERENCE DESIGN

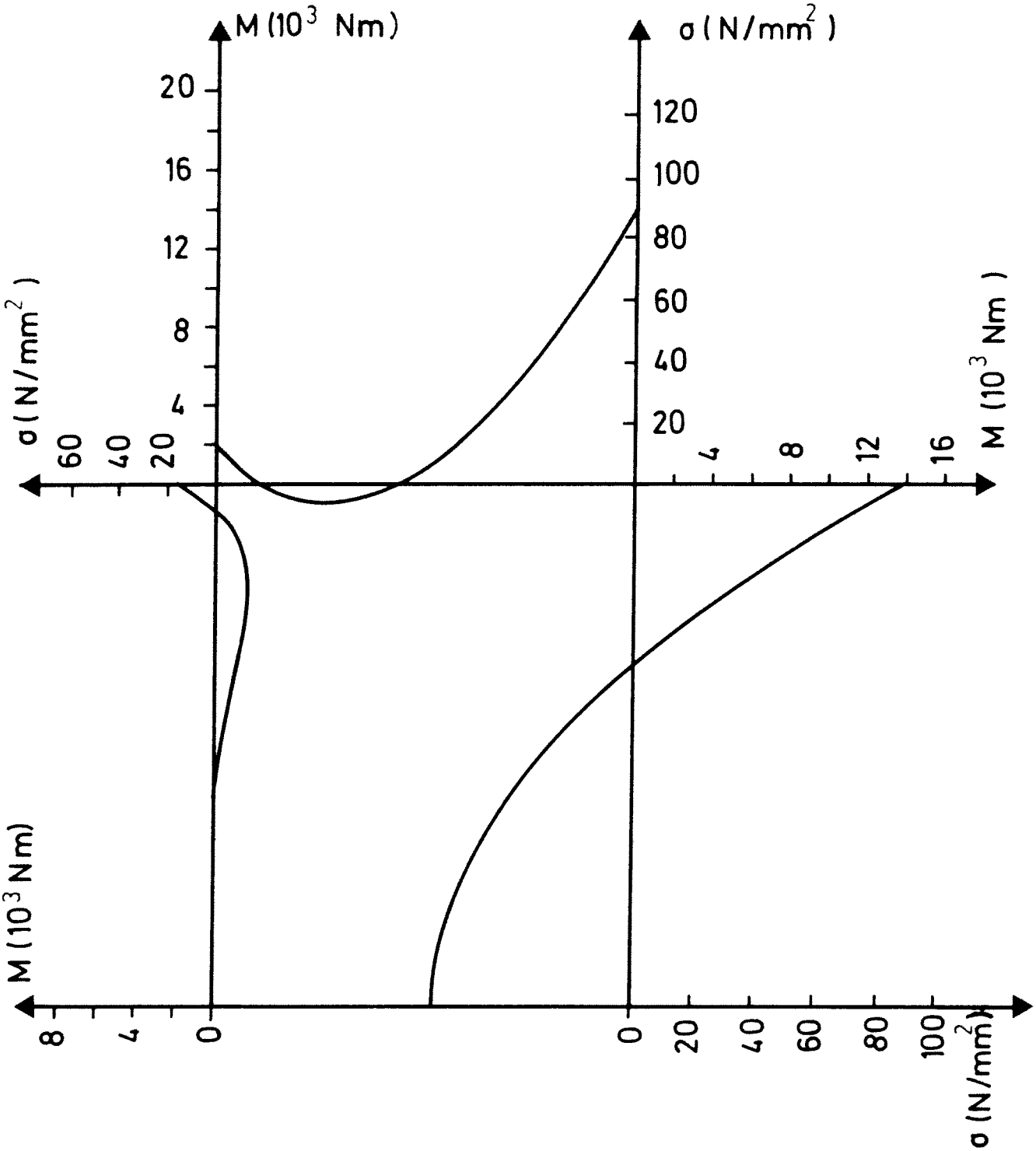

FIG. 2: BENDING MOMENTS AND STRESSES

has 30% higher resistivity than pure copper. The resistive losses in the toroidal field coils at full field amount to 17.1 MW. The coils are water cooled.

In the future, additional stress calculations will have to be performed, using a 2-D finite-element code, in order to obtain more accurate results, and to include the effects of out-of-plane forces.

Section 3 - OH COIL

OH coil currents for ±1.2 volt-seconds are given in Fig. 1. These currents were computed such as to minimize the stray fields within the plasma volume. We assume that 60% of the coil volume consists of copper plus cooling water, the rest being insulation (same as in TCA). The transformer swing is -1.2 to +1.2 volt-seconds, giving 2.4 volt-seconds swing, with a resistive power of 15.2 MW and a temperature rise of 16 °C.

Section 4 - SHAPING COILS

The present design assumes 16 shaping coils. Each coil has the same number of turns and the same cross-sectional area. Since in these coils a relatively large number of turns (~60) has to be fitted into a small cross section, the copper volume fraction will be less than that assumed for the OH coil. A detailed study of the necessary insulation thickness and cooling channel requirements shows that the copper volume fraction will be close to 40%. With a maximum current of 260 kA per coil, we then obtain a current density of 6.5 kA/cm^2 and, taking a pulse length of 1.0 sec, we get a maximum temperature rise per pulse of 25 °C.

Section 5 - VACUUM VESSEL

A vacuum vessel detailed design has not yet been made. A thick-walled vacuum vessel with two insulated poloidal gaps has been

assumed. The minimum distance between the vacuum vessel inner wall surface and the poloidal field coils is taken as 5.5 cm, which is the same as in TCA. The vessel has at least a 5 ms time constant. The question of resistance to disruptive loads remains open.

The shaping coil spacing allows three radial ports of 15 cm i.d. and 22 cm o.d. for the flanges at each of the 16 toroidal positions between the toroidal field coils, allowing use of TCA diagnostics and vacuum hardware, and allowing access for RF heating. Similarly, the lack of coils on the top and bottom of the vessel allows circular or long oval ports for windows.

The limiter system has not yet been designed. However, the probable system is a combination of protective backup limiters at several toroidal planes, with total poloidal coverage, plus coated carbon limiters or pumped limiters at certain selected points, for example at the top of the vessel as in the STARTUP simulations.

Section 6 - CONCLUSION

The concept presented here would appear to be feasible from a technological point of view, but further optimization will be necessary on all systems.

Chapter IV. POWER SUPPLY WAVEFORMS AND MOTOR GENERATOR REQUIREMENTS

In this section, the power supply waveforms for each coil system are specified, and then these waveforms are used to deduce the motor generator requirements. Further optimization is necessary on all systems, and the voltages and currents depend on the detailed design of the coil systems.

Section 1 - TOROIDAL FIELD SYSTEM

The parameters of the toroidal field coil and its power supply are summarized in Table I, and the time-dependent waveforms, measured at the coil terminals, are shown in Fig. 1. A total efficiency of 75% is assumed. To derive motor generator requirements, the energy and power waveforms in the figures need to be divided by the assumed 75% efficiency.

The current in the toroidal current rises from 0.0 to 1.5 sec, equal to the L/R time, under a constant voltage of 432 Volts. The current is then held constant from 1.5 to 2.7 sec with a nearly constant voltage. (The coil will actually heat slightly, increasing the resistivity during the pulse. The actual power will depend on ambient temperature and the cooling system.) At the end of the pulse, the current may be allowed to decay resistively. Alternatively, with supply inversion, some of the 12.7×10^6 Joules may be recovered to save energy and coil heating. With a moderate supply voltage and 75% efficiency, the savings are small.

Section 2 - OHMIC HEATING SYSTEM

For the calculations presented here, we assume that the shaping coils are decoupled from the ohmic coil [see,for example, report GA-A13996], by being connected in parallel across the same number of turns. The ohmic coil is wound with two nearly identical coil groups, each 60 turns, each excluding flux from the plasma, and connected in series to make 120 turns. The 120 turns achieve a reasonable balance

TABLE 1

TOROIDAL FIELD COIL AND POWER SUPPLY

Toroidal Field at R=0.80 m	1.5 T
Number of Coils	16
Number of Turns/coil	6
Total Turns	96
Coil Resistance (96 Turns)	4.4×10^{-3} Ohms
Coil Inductance (96 Turns)	6.5×10^{-3} Henries
L/R	1.5 sec
Current at 1.5 T	62.5×10^{3} Amps
Resistive Voltage (1.5 T)	274 Volts
Resistive Power	17.1×10^{6} Watts
Stored Inductive Energy	12.7×10^{6} Joules
Assumed System Efficiency	75%
Motor Generator Requirements :	
Required Energy	58.8×10^{6} Joules
Peak Power (at 1.5 sec)	36×10^{6} Watts

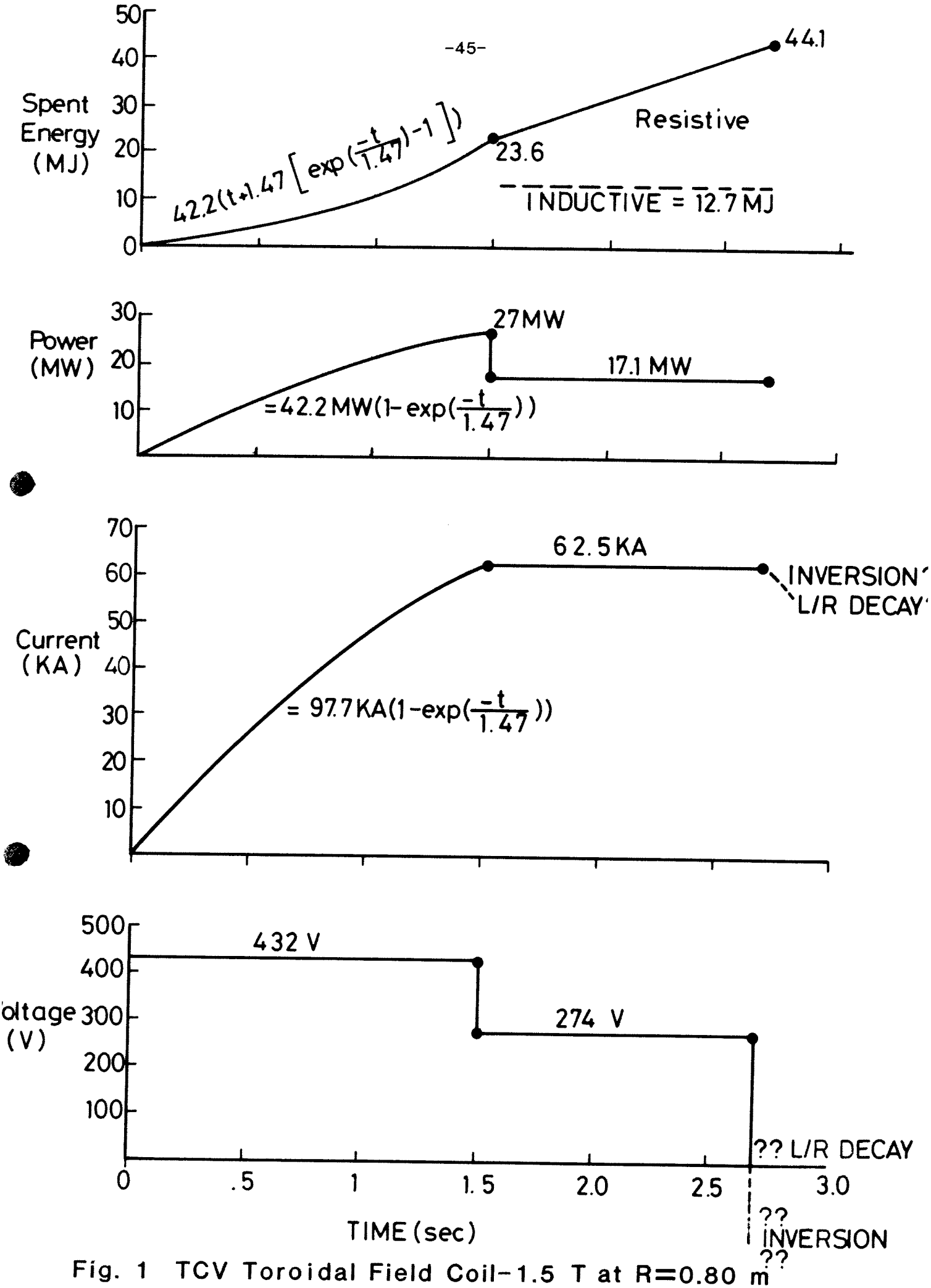

Fig. 1 TCV Toroidal Field Coil-1.5 T at R=0.80 m

Electrical Parameters at Coil Terminal

between coil voltage and current maxima. Also, if any of the 16 shaping coils were connected as series pairs to reduce the number of active circuits, they could be decoupled over the full 120 turns of the OH coil. One important design requirement is a sufficiently large plasma breakdown voltage. The maximum OH supply induced voltage using the OH supply fully on is ±10 volts/turn at the plasma, plus coil resistive voltage. If the inner shaping coils are back biased, then pulsed, a significant breakdown voltage can be added, because the coils are decoupled. The second option is to use a vacuum breaker switch in the OH circuit as an interrupter that briefly shifts the current into a high resistance to generate the breakdown voltage. An ignitron or solid state switch could then be used to short the resistor, and the OH supply would then control the current rise.

We are examining whether it is optimum to connect the shaping coils to only one of the 60-turn halves of the OH coil, or to connect some to one group and some to the other half to balance the return currents. A 60-turn ohmic coil is also an option under consideration.

The coil values and waveforms for a 120 turn OH coil are shown in Table II and Fig. 2. After the toroidal field reaches full current at 1.5 sec and its voltage drops to only the resistive level, the ohmic transformer coil is charged rapidly between 1.50 and 1.65 sec, using the full system voltage available. These 1188 volts (from Fig. 2) were chosen to provide 9.9 V/turn at the plasma, when the OH resistive losses are zero. From 1.65 to 1.70 sec, the OH current is held constant. During this time, the shaping coils and their supplies can be back-biased for additional breakdown voltage or error field correction, and gas can be puffed into the vacuum chamber. At 1.70 sec, the plasma is broken down and the current rise begun. (The inner shaping coils actually have a 1.2 volt-second capability, so only a small back-bias is necessary.) As in TCA, a vacuum-switch, resistor, ignitron network could be used to give a breakdown spike to establish the plasma, instead of shaping coil back-biasing.

TABLE II

OHMIC TRANSFORMER COIL AND POWER SUPPLY

Flux Swing	$-1.2 \rightarrow +1.2$ volt-seconds
Air Core Maximum Field	1.96 T
Number of Turns	2 x 60 = 120
Coil Resistance (120 Turns)	12×10^{-3} Ohms
Coil Inductance (120 Turns)	3.89×10^{-3} Henries
L/R	0.33 sec
Current at +1.2 volt-seconds	36.1×10^{3} Amp
Resistive Voltage (1.2 volt-seconds)	434 volts
Resistive Power (1.2 volt-seconds)	15.7×10^{6} Watts
Stored Inductive Energy	2.5×10^{6} Joules
Assumed System Efficiency	75%
Motor Generator :	
Required Energy	15×10^{6} Joules
Required Peak Power	57×10^{6} Watts

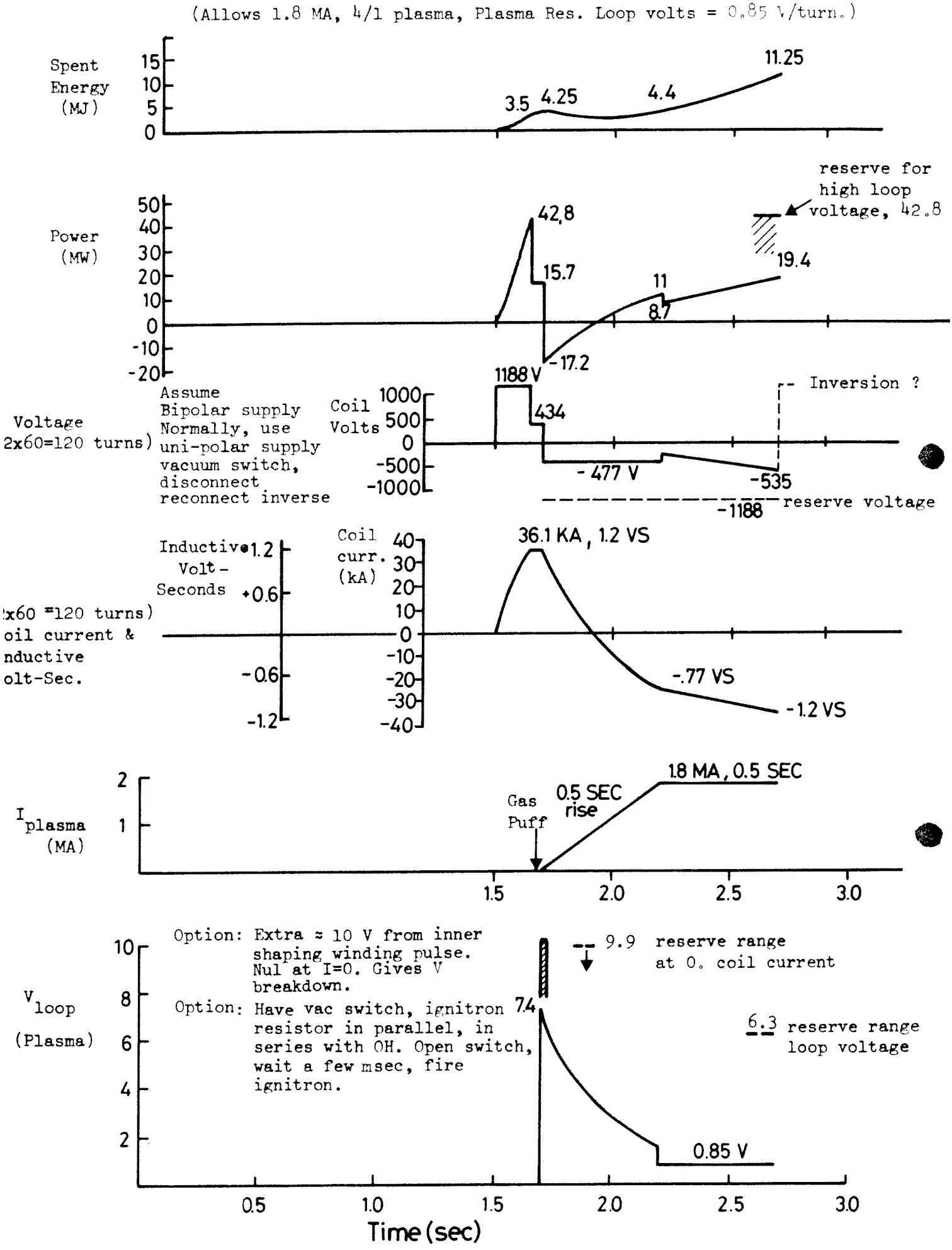

Fig. 2 TCV ohmic system (± 1.2 Volt-seconds)
(At coil terminals)

For the plasma rise, we have chosen a scenario which corresponds to the series of equilibria described in the shaping section, in which the plasma current rises approximately linearly to the maximum current during 0.5 sec. A total of 1.53 inductive volt-seconds are required, plus the resistive plasma voltage (difficult to estimate in this new regime). Here, it is assumed that the plasma achieves a central T_{e0} of 0.9 keV and a resistive loop voltage of 0.85 volts, which is maintained since current is only added to the outer region of the plasma, so there are no losses due to current penetration. In this case, for a linear rise of current during 0.5 sec, a total of 1.97 volt-seconds are expended. This is achieved by applying a constant of -477 volts to the OH coil from 1.7 to 2.2 seconds. Under these conditions, the inductive plus resistive loop voltage in the plasma starts at 7.4 volts and drops as the plasma current increases. After the plasma current rise, the plasma loop voltage is held fixed for 0.5 sec. However, at any time, it may be desirable to apply the full 1188 volt capacity to the E-coil, even at maximum voltseconds. This case determines the peak motor generator requirement of 57 MW for the ohmic system.

With regard to design options for the ohmic coil, an iron core was not chosen because the air core field, even at the reduced 2.4 volt-seconds, is already 2T, covering an area including the toroidal coil volume. Iron cores, especially if saturated, complicate poloidal field analysis and control as well. The ohmic and shaping coil systems were kept separate to minimize the energy and power requirements of the shaping system. Also, there is little direct current cancellation between the ohmic and inner coils, so energy savings would be small.

Section 3 - SHAPING COIL SYSTEMS

The 16 shaping coils each have 60 turns and each has its own controlled power supply. The coil parameters are summarized in Table III, and the resistive power waveforms in Fig. 3. Since the total externally supplied inductive energy is only 0.4 megajoules, one design possibility is that some fraction of this energy is stored in

TABLE III

SHAPING COILS

Number of coils	16
Turns per coil	60
Area per coil	0.01 m^2
Copper fraction	0.4
Maximum current/coil	260/60 = 4.33 x 10^3 Amps
Externally supplied inductive energy in all coils	0.4 x 10^6 Joules
Peak resistive power in all coils	8.9 x 10^6 Watts
Dissipated energy total	6.4 x 10^6 Joules

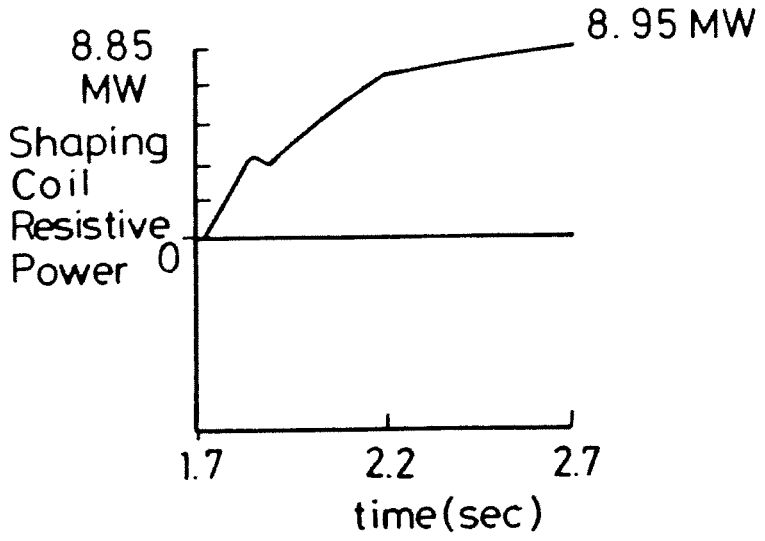

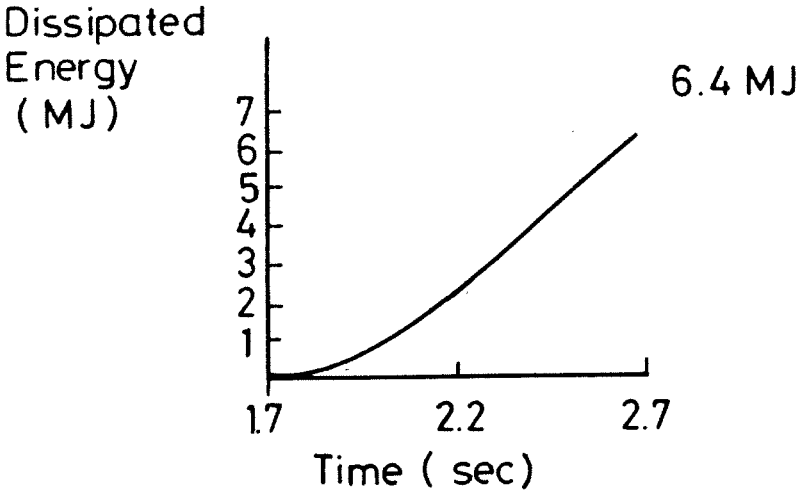

POWER AND ENERGY SUMMARY

TIME

1.7 → 1.704 Fast breakdown spike, no external power used.

Time	Supply Power	Supply Energy	MG (75%) MG Energy	MG(75%) MG Power
1.7-2.7 sec.	8.9 MW	6.4 MJ	8.6 MJ	11.8 MW

Fig. 3 Shaping Coil system. - Resistive Power needed

capacitors for each supply. Very high power for feedback would be available on a time scale faster than or comparable to the vacuum vessel skin time, i.e. milliseconds. If capacitors were used, they could be topped up by a d.c. supply connected to the motor generator, in order to supply the coil resistive losses. This would avoid any peak power on the motor-generator. The detailed waveform of a representative shaping supply is shown in the section on plasma shaping. The choice of technology for the shaping coil supplies will depend on maximum coil voltage, which in turn depends on the choice of number of turns and shaping power requirements.

Section 4 - RESERVE FOR AUXILIARY HEATING AND/OR OHMIC SYSTEMS

A reserve capacity is added to the motor generator requirements for auxiliary heating and/or for a future increase of volt-second capability, if required.

For an auxiliary heating reserve, if we assume that 5 MW of plasma heating are required for 0.5 sec, and a generator to plasma efficiency of 25%, this gives 20 MW at 10 MJ of energy. The method of heating, possibly by Alfven or Ion Cyclotron waves, has not yet been specified.The AFCO system can be used for initial studies, but it has a limited pulse length due to capacitive energy stage. Its capacitors could be topped up for 0.5 sec by an external d.c. supply.

Also, 20 MW represents a reserve for augmenting the volt-second capability, if this should be seen to be necessary. At 75% efficiency, these reserve requirements for the motor generator are :

Stored energy : 13.4×10^6 Joules

Power extracted : 26.6×10^6 Watts.

Section 5 - MOTOR GENERATOR REQUIREMENTS - Preliminary estimate.

The minimum requirements for the motor generator are shown in Table IV, and may be summarized as : 95.5 Megajoules of extractable energy, and 118.2 Megawatts of extracted power. The largest energy requirement, 58.5 MJ is for the toroidal coil, and the largest peak power, 57 MW, is for the ohmic supply.

TABLE IV

TOTALS FOR MOTOR GENERATOR REQUIREMENTS - Preliminary estimate

Extracted Energy :	Toroidal Coil	= 58.5 MJ
	Ohmic Coil	= 15.0 MJ
	Shaping System	= 8.6 MJ
	Reserve for Auxil. Heating or Ohmic Upgrade	= 13.4 MJ

Required : Total Extractable Energy = 95.5 Megajoules

MG Peak Power - Occurs near pulse end.

Toroidal Coil Worst case : B_T=1.5 T	→ 22.8 MW	Note : Peak extracted power, not simultaneous 36 MW (when B_T ramped)
Ohmic Coil Max Loop Voltage at Max I_p	→ 57 MW	57 MW
Shaping system	→ 14.1 MW	11.8 MW
Reserve for Aux Heating or ohmic upgrade in use	→ 26.6 MW	26.6 MW

Required : Total worst case peak → 118.2 Mega-Watt

Note : In normal operation, the MG is always discharging, even during the current spike unless the OH and Toroidal Field are inverted to recover some fraction (75% eff. + coil resistive losses) of 12.7 MJ in TF coil and 2.5 MJ in ohmic coil.

CHAPTER V. DIAGNOSTICS, DATA ACQUISITION, MACHINE CONTROL

Section 1 - MAGNETIC DIAGNOSTICS

The TCV magnetic diagnostics will be designed for the purposes of machine control and for the analysis of elongated discharges. Signals must be provided as an input to the positional and shaping feedback system. The flux loops and magnetic field probes are used to determine the plasma current, magnetic flux, and the spatial derivative of the flux as near to the plasma as possible, in order to determine the shape and the moments of the current distribution. This will require the use of internal discrete coils and flux loops located in the vessel, which may be extrapolated to determine the value of flux on the plasma surface. These signals may then be combined as described in the section on shaping control.

Magnetic oscillations will be measured at low frequency with internal discrete coils located in stainless steel tubes. RF-wave-fields and OH-magnetic fluctuations will require the use of unshielded coils. Diamagnetic coils with compensating loops are included in the machine design to solve the problems of stray field compensation and mechanical deformation.

The magnetic coils must provide sufficient information for the numerical reconstruction of 2-D equilibria. The methods of reconstructing the equilibria from flux loops and magnetic probe signals will be the same as described extensively by other tokamak groups. The MHD analysis code will run on the central EPFL computer.

The coils must be of robust construction and included from the beginning in the design of the vacuum vessel. A sufficiently large number of poloidal planes will be equipped with magnetic coils to fulfill the requirements in control and analysis. The coil system should provide enough redundancy for furnishing feedback signals and input signals to an equilibrium reconstruction code [Computer Physics Reports, 1 (1984), Numbers 7 and 8].

For safety and ease in the operation, it is beneficial to separate the coils used for the operation and the coils used for the analysis. There must be enough coils for a full poloidal and toroidal mode analysis. In case of failure, the replacement of such coils would be difficult. Therefore, spare coils have to be foreseen.

A large number of different combinations of individual coil signals may be formed. This will be done in the control room via summing amplifiers, integrators, or by digitally. These combinations can be used for control and analysis purposes.

The system must also be sufficiently versatile to cope with the evolution in control concepts that such a project will certainly undergo, as part of its experimental programme.

Section 2 - OTHER DIAGNOSTICS

Almost all TCA diagnostics and electronics will be usefully available for TCV. Electromagnetic diagnostics are discussed in the previous section.

In Table 1 we list the minimum TCV diagnostics for commissioning, marking where they can be rebuilt from TCA and where they are not useful at high density.

The major problem will be the reconstruction in 2-D of the measured quantities. Many multi-channel devices will be needed, and luckily we already possess Soft-X, Hα, an 8-channel interferometer and Bolometry in this form. Considerable use of quasitangential fish-eye optics may well be essential.

Table 1

Diagnostic	From TCA	High density
NPA (5 ch)	T	NU
NPA (high energy)	T	NU
Thomson scattering	T(1)	T
X-Ray Flux	T	T
X-Ray Spectrum (SiLi)	T	T
2 mm μ wave	T	NU
1/2 mm FIR (8 ch)	T	T(2)
VUV monochromator	T	T
Bolometer (16 channel)	T	T
Neutrons	T(3)	T
Multi-H_α	T	T
Visible monochromator	N	N
Video recording (+filters)	N	N
Visible Bremstrahlung	T(4)	T

Notes : T : Transferable form TCA

NU : Not useful at high density, but usable at low density operation

N : Needed.

1) Possibly inadequate system

2) Useful up to 5 x 10^{14} cm^{-3} (? some chords)

3) One detector available out of 3-4 necessary

4) More channels necessary

Section 3 - DATA ACQUISITION AND LOCAL COMPUTER

The TCA philosophy of separating machine control and data acquisition will be continued. The present TCA system is extremely simple and works well. We would therefore retain part of the software and hardware we have acquired. We now have 208 x 1 kByte x 12 bit ADC channels used as slow/medium speed ADC's. They would be retained for slow monitoring (≈khz for TCV, i.e. comparable to shell-time). We posess a limited number of faster 8-bit ADC's in CAMAC which would be extended for faster sampling. More specific requirements cannot be sensibly defined before the diagnostics are conceived. Depending on the chosen data acquisition rates, the present system might be a little too slow for TCV, and data concentrators would be purchased to avoid interfacing directly to the central computer.

The PDP 11/60 presently in use on TCA would eventually be replaced on TCV, even if used for initial commissioning. Its addressable memory is too small to manipulate efficiently the larger quantity of data produced by TCV, partly due to its longer pulse-length and partly due to the regular use of all available 2-D diagnostics. The choice of a suitable machine must be left as late as possible, as must its configuration, due to the predictable rapid developments. It is important that the replacement computer be at least as rapid as the PDP 11/60.

We shall acquire more control information than on TCA as few subsystems were designed with this in view on TCA. This may or may not be permanently stored.

The philosophy of fully central data storing and archiving will be maintained on TCV where possible. One requirement shown by TCA will be the preparation of an independent vector-to-raster generator to discharge the local computer of this part of its work.

Section 4 - MACHINE CONTROL

The present philosophy of the TCA surveillance system is considered to be correct and will be maintained. No overlap will exist between control and data acquisition. Subsystems will be under remote or local control with central control mimicking locally. This has enabled for TCA, and will enable for TCV, total flexibility for construction, commissioning, testing and repair. Limited status reporting will be provided centrally, sufficient to operate the machine under normal conditions; full information will be available locally. Responsibility for subsystem safety and subsystem access will both be provided locally.

Considerable use will be made of fibre-optic transmission for both data and timing systems. The machine sequence will be under autonomous timer control, as on TCA during the actual shot. We shall require a soft-abort system on many systems to avoid excessive power dissipation in particular subsystems after a plasma or machine fault. We shall avoid the philosophy that requires correct functioning of both hardware and software to avoid damage, relying on separately protected subsystems, with the maximum of autonomy. In order to achieve a high reliability of the subsystems, duplication of important control signals will be provided.

On TCA positional feedback, gas feed, density feedback and current feedback/control are defined by arbitrary waveforms. This system will be replaced by a more sophisticated system, allowing more functions to be pre-determined. At present verification is performed by the operator. This will be modified to allow computer simulation of the plasma shot performance prior to the shot, to verify all the demand signals. Interaction between central control and the computer will be via the standard acquisition. The possibility will therefore be available for storing the demand waveforms on an operation library, but nonetheless retaining simple modification procedures.

Interlock surveillance will be carried out independently of the control computer system, as is the case on TCA. Yes/No information is then available to the central computer, as on TCA. Local interlocks are also included in the local subsystem, creating a simple tree-system, simple for commissioning.

CHAPTER VI. PLASMA PARAMETERS AND HEATING

Section 1 - PLASMA PARAMETERS WITH OHMIC HEATING

We do not have suitable scaling laws with which we can predict the plasma parameters of strongly elongated plasmas such as TCV at 4/1 elongation. Nevertheless, we try to use the scaling laws derived from experiments of modest elongations and from the little theory available, in order to show the magnitude and uncertainty of the extrapolation as well as to predict at least possible ranges of operation.

The key parameter which we would like to determine is the maximum current which can be accommodated without major disruption. It is accepted that $q_a \approx 2$ is an operational limit of circular cross-section tokamaks which do not have specific features to cross it and we take this as our limit. It translates into a limiting current

$$I_{cm} = \pi a^2 B/\mu_0 R.$$

For a moderately elongated plasma it has been found in Doublet III that one can work down to $q_I \sim 2$ and even slightly lower, where q_I is the INTOR definition

$$q_I = q_a(1 + K^2)/2,$$

q_a being the value calculated assuming the plasma is circular with the radius a. This limit $q_I \sim 2$ is equivalent to a maximum current of

$$I_I = I_{cm}(1 + K^2)/2.$$

According to this relation, the limiting current would then increase from about 150 kA to 1.3 MA at full elongation. But if $q_a = 2$ for a circular plasma has some theoretical backing, the limit $q_I \approx 2$ has none, since q_I is the safety factor of an elliptical plasma having the same elongation and constant current density.

Another safety factor has been introduced by D.A. D'Ippolito et al., which, for a racetrack, is related to q_a by

$$q^* = q_a(1 + 2\ (K-1)/\pi).$$

If one assumed that $q^* \approx 2$ is the true limit, the corresponding current would be

$$I^* = I_{cm}(1 + 2\ (K-1)/\pi)$$

which is only about 450 kA at full elongation. This q^* was introduced in relation with a theory of the stability of skin-current tokamaks which predicts the stability limit at $q^* = 1$ for a circular plasma and about 0.75 for a racetrack of 4/1 elongation. Since $q^* = 1$ for a circular plasma is not the observed limit, we do not know if it is reasonable to take $q^* = 2$ as the limit for the racetrack. Since this theory does not predict correctly the behaviour for small elongations or the parametric dependence of the β limit on current, we shall ignore this prediction.

By using the rotational transform q_ψ instead of q_a, we obtain another method to evaluate the maximum current provided one assumes $q_\psi \approx 2$ as the limit. This was done in the equilibrium calculations and it led to a current of about 1.7 MA, much larger than any of the other predictions. We have not been able yet to find with ERATO the MHD stability limit, even at $\beta = 0$, but the calculations are now in progress. But whatever the final value calculated with ERATO, it should be considered as just one more prediction until it has been verified experimentally. This value of 1.7 MA should be considered as an extreme limit.

The limiting volume averaged β observed in all tokamaks with sufficient auxiliary heating is given by

$$\beta_{max} = C(\mu_0 I/aB_T) \equiv CI_N.$$

where the constant C is around 2.5 to 3% for the bulk plasma and maybe

3.5% with inclusion of the beam contribution. This law has been verified for circular and moderately elongated plasmas. It has not been verified neither theoretically nor experimentally above an elongation of about 2. Using it, nevertheless, we find that β_{max} varies from about 1.7% at 150 kA(q_a = 2 for a circular plasma) to about 20% at 1.7 MA, the maximum value of the current one can reasonably expect in a 4/1 racetrack plasma.

For small elongations the scaling law seems to remain valid up to the limiting current. Neither theoretically nor experimentally has it been possible to follow an eventual gradual drop in β as the current limit is approached. This may be different at higher elongations but we did not find theoretical or experimental data relevant to this question.

The density limit is another crucial parameter. J. Hugill has given a law

$$\bar{n}_{19max} = 20B/Rq_a$$

for circular plasmas which can be rewritten in various forms, generalizing to very different expressions for non-circular cross-sections. For example, the expression above can be rewritten in the form

$$\bar{n}_{19max} = 10\mu_0 \langle j \rangle$$

which generalizes immediately to any cross-section. It leads to a decreasing density limit with increasing elongation at constant current. An expression of the same form but with a smaller coefficient has been used to analyze the first JET results successfully, but in smaller devices (and TCV is small) this trend is definitely wrong.

Another generalization proposed by J. Hugill consists of expressing the density limit in terms of the β limit

$$\bar{n}_{19max} = 10/\pi \; B_\phi/a \; I_N = 10/\pi C(B_\phi/a)\beta_{max}.$$

It then predicts that the density limit is independent of elongation but increases linearly with the current, parallel to the β limit. This relation fits the experimental data of small devices up to moderate elongation in particular the Doublet III discharges with the record β of 4.6%.

Using this last expression, one obtains for the density limit:

$\bar{n}_{max} = 1.9 \times 10^{20}$ m^{-3} for the circular case
$\bar{n}_{max} = 2.2 \times 10^{21}$ m^{-3} for the full elongation and 1.7 MA.

Since this density scales as the current, a reduction of the current reduces the last number in proportion. The uncertainty in the maximum current translates into just as large an uncertainty on the density limit which only experiment can resolve.

This density limit will probably not be reached in an ohmic plasma just with puffing. Pellet injection may be one method to reach it. But a density about half of the $q_\psi = 2$ limit, corresponding to about 5 Murakami units, is reached in tokamaks of the size of TCV with puffing only.

The energy confinement time can be estimated by the scaling law

$$\tau_E = 0.192\, \bar{n}_{20}\, R^{2.04} a^{1.04}$$

strictly validated for circular plasmas [Plasma Physics and Controlled Fusion 26 (1984) 20] but in the absence of any experimental evidence that moderate elongation brings a change in the scaling, we shall use it. For our parameters it gives

$$\tau_E \approx 20\, \bar{n}_{20} \text{ msec.}$$

For 1.7 MA, it would lead to a confinement time of 0.44 sec. For a more realistic current of 1.2 MA, and a density of 80% of the Hugill limit, τ_E is still 0.23 sec. At high currents in a racetrack configuration, the neoclassical ion thermal conductivity losses should be small.

There remains to estimate the range in which we can hope to find the resistive loop voltage to determine volt-second requirements.

Let us designate by $\langle A \rangle$ the volume average of A and by A_0 the value on axis. In circular plasmas, the current density on axis j_0 is determined by the condition $q_0 \sim 1$. In very elongated cross-sections there may be also such a condition which fixes j_0, so that it is convenient to express the loop voltage V in terms of j_0 as

$$V = 2\pi R_0 \eta j_0 = 1.26 \times 10^{-7} \, j_0 Z_{eff} \, T_{eokeV}^{-3/2}.$$

From the power balance equation

$$VI = 3/2 \; X \; \langle n_i k_B T_i + n_e k_B T_e \rangle / \tau_E,$$

where X is the plasma volume. Replacing τ_E and V by their expression one obtains

$$T_{eo} = 6.3 \times 10^{-6} (I j_0 Z_{eff} / fX)^{2/5},$$

where f is a form factor defined as

$$f \equiv \langle n_e T_e + n_i T_i \rangle / n_e T_{eo},$$

Substituting

$$V \approx 8 (j_0 Z_{eff})^{2/5} \; (fX/I)^{3/5}.$$

For the circular plasma with $q_a = 2$, $I = 150$ kA, $j_0 = 3 \times 10^6$ A/m^2 ($q_0 \equiv 1$), $f \approx 0.7$, $X = 0{,}5$ m^3, $Z_{eff} = 1$.

$$T_{eo} \approx 0.44 \text{ keV}, \qquad V \approx 1.3 \text{ V}$$

which are very reasonable values. The dependence of V on the current is weak and is countered in part by a decrease of f which reflects increased peaking.

With elongation, the current hopefully should increase more than the volume. The current density j_0 will either remain the same or increase depending on the elongation of the central flux surfaces. In the example shown in Fig. 10 with 4/1 elongation and 1.7 MA, j_0 is twice the circular value. One can reasonably expect that j_0 will not exceed four times the circular value. One can then expect a rise of T_{eo} and little change in the loop voltage. The values for the 4/1 elongation and 1.7 MA example are T_{eo} = 0.9 keV and $V_L \approx 0.9$ V. This is typical of what is expected if the scaling law for τ_E remains applicable and is consistent with our assumptions on volt-second requirements.

Section 2 - AUXILIARY HEATING

Neutral beam heating has not yet been considered for TCV because of difficulty of access and high cost. Also, the choice of energy depends on the maximum obtainable density.

Lower Hybrid heating has not yet been considered in detail.

For Electron Cyclotron Heating, the low magnetic field of TCV rules out use of both the first and second harmonics (40 and 80 GHz). The third harmonic, restricted to densities less than 2×10^{14} cm^{-3}, remains a possibility especially since the CRPP has a gyrotron development programme for the frequency 120-150 GHz. A hot, dense target plasma would be required to absorb the wave, and only first and second harmonic heating has been extensively studied.

For Ion Cyclotron Resonance Heating, as the wavelengths of the excited waves increase, the geometry of TCV begins to be important. ICRF, however, should have no obvious difficulty in adapting to either the shape or the high densities at which second harmonic heating is generally preferred.

Due to the theoretical, experimental and technological expertise at the CRPP, the Alfvén frequency range (1-5 MHz) would appear attractive. However, at these large wavelengths the global nature of the excited waves plays a vital role so that AWH will be sensitive to the unique geometry of TCV. At present, it is difficult to propose an appropriate range of toroidal and poloidal wavelengths and thus define a frequency or a suitable antenna structure since the highly elongated cross-sections will certainly require a different solution than in TCA. Preliminary theoretical work is underway. It should be noted that the high power, variable-frequency AFCO system under construction for TCA will be available for TCV.

In conclusion, ICRF and AWH remain the preferred possibilities as additional heating techniques for TCV. Both require further study - ICRF in its detailed application and AWH in its application to highly elongated cross-sections. Both have questions of edge dissipation, associated impurity release, and changes to particle and energy confinement, which present experiments will continue to address, so that a more informed decision can be made later. Provision has been made in the plasma shaping and vacuum vessel design for the addition of heating antennae.

CHAPTER VII. BILIOGRAPHY

Section 1 - BIBLIOGRAPHY

Plasmas with very high elongation have been experimentally produced for many years in Belt Pinches [1-7] and in tokamaks [8-10]. There is an area of intermediate machines going from elongated screw-pinches to shock-heated elongated tokamaks [11-15]. A new machine in the SPICA series is continuing these studies.

Plasmas in these machines tend to be transient due either to the high density and low electron temperature resulting in current peaking and shrinkage of the current channel [16-17] or most simply due to a lack of active poloidal shaping and stabilizing system, as in the Finger Ring tokamak series, for example [8]. The Finger-Ring tokamak was chosen to have triangularity facing away from the centre-line to help to satisfy the Mercier necessary and Lortz sufficient stability criteria.

Elongated plasmas have been obtained on a longer timescale. Doublet plasmas with 3/1 elongations [18] have been produced in D-III, but due to peaked current profiles, the two magnetic axes were nearly circular, and were linked by a relatively small (<25%) fraction of common flux. On the other hand, with flat current profiles, plasmas have been formed in the upper half of Doublet III with a single magnetic axis, with elongations up to 2.1/1 [19,20]. With hollow profiles, the central surface has an even higher elongation, 2.4/1, leading to a central q value higher than that at the edge. These plasmas lasted 10's of milliseconds, gradually shrinking as the current increased, since the safety factor at the edge was q = 10. Extensive studies of vertical stability of steady-state plasmas with $K < 1.8/1$ and peaked current profiles have been made in Doublet III [21]. These studies indicate that flattening the current profile allows higher elongations, especially with feedback control. TOSCA has been used to study the effects of shaping the plasma cross-section into an elliptic, a triangular, and a D-shaped form [22]. ISX-B has also studied elongated cross-sections.

With improved plasma cleanliness and control techniques, many tokamaks can now produce flat-top discharges, with low-q≈2 and flat current profiles. These flat profiles should make it possible to maintain highly elongated plasmas, which is one of the principal goals of the TCV experiments.

At the last IAEA Conference (London, September 1984), in a special session on high-beta tokamak discharges, one conclusion was that shaping is an important remaining issue to be studied more extensively.

At the same Conference, some interesting studies were presented with moderate elongations. Toroidal screw-pinch configurations with elongated cross-sections are studied in ETL-TPE 2 [14]. A very thorough work on β-limits has been undertaken by the D-III team with elongations up to 1.8 and with strong NBI. This makes use of the increased current allowed with elongation [23]. JET has presented results with stable elongations up to 1.63. Improvements in disruption control will come from an increased speed of amplifier response and from active shape control. This problem is crucial on the way to full performance in JET [24]. The recent Princeton Bean Experiment (PBX) has achieved high beta plasmas by indenting the plasma, supplementing a moderate vertical elongation. Very positive results have been obtained [25]. Miller and Moore [26] in a theoretical paper show that beans with vertical elongations may have even better properties.

Theoretical aspects have been developed in the PBX-paper [25], D-III Paper [23], a JAERI-Paper [27], and a PPPL paper [28].

Even though elongation is used at present in the largest tokamaks and continues to be studied in rather small devices, one notices that no experiment is presently aiming at studying relatively steady-state, highly-elongated cross-sections in a tokamak of reasonably large size.

Most numerical studies of plasma MHD stability have up to now been performed on plasmas with moderate elongations of less than 2.0.

A study has been made [33] of the validity of the CRPP scaling at moderate elongations and small aspect ratio (2.75) with the same technique and assumptions used to find the scaling. The aim was to choose the parameters of the R-Tokamak, a project of the Nagoya University. The conclusion is that $q \approx 2$ continues to define the limiting current up to an elongation of 2, but the β has an optimum at an elongation of 1.8, then decreases as the elongation increases. The original choice of current and pressure profiles did not work at high elongation and they were replaced by gaussian profiles, with pressure more peaked than current. From studies made at the CRPP [unpublished], we know that the kink limit, which was the critical one in the quoted study, can be improved by having the pressure profile wider than the current profile. The shape was always elliptical with a small triangularity. We are interested in racetrack configurations which have very different q profiles.

The ERATO [29] code at Lausanne as well as the equilibrium code which provides the input had to be modified to handle such highly elongated equilibria. The stability code has resolution problems due to increased elongation, particularly due to high shear at the edge. Greater flexibility had to be introduced into the source functions to allow greater variety of q profiles. There are no results yet.

Chance, Furth, Glasser & Selberg [28] have studied the ideal and resistive-MHD stability of one-dimensional tokamak equilibria, which correspond to racetrack equilibria with the end effects ignored. They find very favorable stability properties, and conclude that it should be possible to realize these benefits in a realistic system with finite ends. The stability properties of modes localized in the end sections may be stabilized by special tailoring of the end sections [30].

Using a surface current model, an extensive theoretical study of the stability of high beta tokamaks was carried out by Friedberg, Haas, Marder, Grossmann, and Goedbloed (1973-1976) at Los Alamos. These results are reviewed by Bateman [31]. Marder concluded that a racetrack geometry could lead to improvement in critical beta. For

large aspect ratio toroidal results, the maximum critical beta increases as elongation is increased to 2.2/1 and decreases above this, and additionally, the value of q must be increased. Analytical work by Laval, Pellat, and Soulé [32] on kink modes in elliptical plasmas indicate that a uniform current profile leads to the broadening and overlap of bands of unstable q-value as the elongation is increased, but that peaked profiles suppress modes with higher harmonics.

It is clearly difficult to draw conclusions from this previous work. There are obviously potential problems with very highly elongated plasmas, but the range of adjustable parameters, i.e., shape, height, current and q profile, pressure, etc, is large, and there does seem a strong possibility of increasing beta with elongations greater than the experimentally explored range of 1-2.

Section 2 - REFERENCES

Belt Pinches

[1] H.J. Belitz et al., IAEA Conf., Madison (1971), Vol. III, 179

[2] F. Hofmann, Nuclear Fus. 15 (1975) 336.

[3] G. Becker et al., Proc. 7th Conf., Innsbruck (1978), Paper IAEA-CN-37/U-2, and G. Becker et al., 8th EPS Conf. on Plasma Physics, Prague (1977), Vol. I, 76, and O. Gruber et al., 6th IAEA Conf., Berchetsgaden (1976), Vol. I, 311.

[4] K.H. Dippel et al., Proc. 5th Conf., Tokyo (1974), Paper E4-2.

[5] F. Hofmann, L. Bighel and J.M. Peiry, Proc. 7th EPS Conf. on Plasma Physics, Lausanne (1975), Vol. I, 137 and references therein, and J.M. Peiry et al., 8th EPS Conf. on Plasma Physics, Prague (1977), Vol. I, 75.

[6] E.J.M. van Heesch, A.E. Prinn and A. Verheul, 8th EPS Conf. on Plasma Physics, Prague (1977), Vol. I, 73.

[7] T. Tamura et al., 7th IAEA Conf., Innsbruck (1978), Vol. II, 55.

Old Tokamak experiments

[8] A.V. Bortnikov et al., Proc. IAEA Conf., Tokyo (1974), Vol. I, 147.

[9] H. Toyama, S. Inoue, K. Itoh et al., IAEA Conf., Berchtesgaden (1976), Vol. I, 123 and H. Toyama et al., 7th IAEA Conf., Innsbruck (1978), Vol. I, 365.

[10] T. Okhawa et al., IAEA Conf., Tokyo (1974), Paper CN-33/A10-1, Vol I, 281.

Intermediate machine

[11] A. Aydemir et al., 7th IAEA Conf., Innsbruck (1978), Vol. II, 78.

[12] R.M.O. Galvao et al., 8th IAEA Conf. Bruxelles (1980), Vol II, 325, (Paper CN-38/L-4-1).

[13] C.K. Chu et al., ibid, Vol.II, 339, (Paper CN-38/L-4-2), and C.K. Chu et al., 9th IAEA Conf., Baltimore (1982), Vol. II, 321.

[14] S.Kiyama et al., 10th IAEA Conf., London (1984), (Paper CN-44/A-VI-3).

[15] C.K. Chu et al., IAEA Conf., Berchtesgaden (1976), Vol. I, 511.

Following references

[16] F. Hofmann, Nucl. Fus. 14 (1974), 438.

[17] D. Berger, R. Gruber, F. Hofmann and V.K. Nguyen, Nucl. Fusion 17 (1977), 1095.

[18] J.C. Wesley et al., Plasma Physics and Controlled Nuclear Fusion 1981, Proc. 8th Int. Conf. Brussels (1980).

[19] F.B. Marcus, D.R. Baker and J.L. Luxon, Nuclear Fusion 21 (1981), 859.

[20] F.B. Marcus et al., Proc. 10th European Conf. Cont. Fusion and Plasma Physics, Moscow (1981).

[21] H. Yokomizo et al., Proc. 9th IAEA Conf. Baltimore (1982).

[22] K.M. McGuire, D.C. Robinson, A.J. Wooton, IAEA Conf. Vienna (1979) IAEA-CN-37/T-1-1

[23] R.D. Stambaugh et al., ibid, and IAEA Conf., London (1984), Paper CN-44/A-IV-2-1.

[24] P.H. Rebut et al., ibid, Paper CN-44/A-I-1.

[25] M. Okabayashi et al., ibid, Paper CN-44/A-IV-3.

[26] R.L. Miller and R.W. Moore, Phys. Rev. Lett. 43 (1979) 765

[27] T. Tuda et al., IAEA Conf. London (1984), Paper CN-44/E-III-4.

[28] M.S. Chance, H.P. Furth, A.H. Glasser and H. Selberg, Nucl. Fusion 22 (1982) 187.

[29] R. Gruber et al., Comput. Phys. Comm. 21 (1981) 323.

[30] Greene, Chance, Nucl. Fus. 21 (1981) 453.

[31] R. Bateman, MHD Instabilities, The MIT Press, Cambridge, Massachusetts (1978).

[32] G. Laval, R. Pellat, and J.S. Soulé, Phys. Fluids 17 (1974) 835-845.

[33] H. Naitou et al., Report IPPJ-694 (Sept. 1984), Inst. of Plasma Physics, Nagoya University.